

MONITORING FLOODPLAIN RESTORATION USING UAV LIDAR AND
2D HYDRAULIC MODELING ON THE GREENWATER RIVER, WASHINGTON

by

Brian Zierdt

A Thesis
Submitted in partial fulfillment
of the requirements for the degree
Master of Environmental Studies
The Evergreen State College
September, 2018

© 2018 by Brian Zierdt. All rights reserved.

This Thesis for the Master of Environmental Studies Degree

by

Brian Zierdt

has been approved for

The Evergreen State College

by

Edward A. Whitesell, Ph. D.
Member of the Faculty

Date

ABSTRACT

Monitoring Floodplain Restoration Using UAV Lidar and 2D Hydraulic Modeling on the Greenwater River, Washington

Brian Zierdt

Anthropogenic changes to the landscape have reduced both fish habitat and the natural flood protection of streams and rivers. Shifting trends in river discharge also present an increased risk to salmon survival, and highlight the importance of floodplain restoration projects to boost resiliency to climate change. Lidar-derived topographic data input into a hydraulic model can be utilized to quantify the benefits of floodplain restoration. UAV lidar technology can provide more detailed topographic outputs than conventional lidar flown with manned aircraft. This study used both conventional and UAV lidar within a 2D hydraulic model, run using HEC-RAS 5.0.3, to analyze how well the Greenwater River Floodplain Restoration Project achieved proposed floodplain reconnection and velocity reduction goals. Second, it explores the potential benefits of using high-resolution UAV lidar. Results show that the Greenwater River restoration had a positive impact on project metrics, with an 8.2% gain in floodplain inundation area and an 8.5% reduction of velocities in the main channel at the 100-year flood. Dense tree canopy in the project area reduced the potential 1 cm detail of the UAV lidar output, resulting in a 1-foot DEM. A comparison of model results run on the native post-project terrain and a downsampled 3-foot terrain, the resolution of the pre-project data, resulted in very little change in spatial patterns, with a 1.3% reduction of inundation area and a 0.5% reduction in velocities across the floodplain at the 100-year flood. Benefits of high-resolution UAV lidar for the production of detailed roughness values and the assessment of fine-scale habitat features is discussed, although the latter would likely require the capture of blue-green bathymetric lidar and not only near-infrared lidar captured for this study. UAV lidar is ultimately shown to be a cost-effective method of obtaining a highly detailed topographic model for smaller projects of a few 100 acres or less.

Table of Contents

1.0 INTRODUCTION	1
2.0 LITERATURE REVIEW	8
2.1 Introduction.....	8
2.2 Monitoring the Effectiveness of Stream Restoration.....	9
2.3 Climate Change and Salmon.....	12
2.4 Hydraulic Modeling Using Lidar.....	15
2.5 Summary	20
3.0 METHODS	21
3.1 Introduction.....	21
3.2 Study Area	22
3.3 Data	23
3.3.1 Lidar	24
3.3.2 Discharge and Basin Statistics	28
3.3.3 Aerial Imagery	31
3.3.4 Land Cover and Manning’s n Roughness Values.....	33
3.4 Modeling.....	36
3.5 Results Analysis.....	40
4.0 RESULTS	41
4.1 Introduction.....	41
4.2 Inundation Area	43
4.2.1 Inundation Area - Mean Annual Minimum	45
4.2.2 Inundation Area – Bankfull	46
4.2.3 Inundation Area – 5-Year	47
4.2.4 Inundation Area – 10-Year	48
4.2.5 Inundation Area – 25-Year	49
4.2.6 Inundation Area – 50-Year	50
4.2.7 Inundation Area – 100-Year	51
4.3 Flow Velocity.....	52
4.3.1 Flow Velocities – 10-Year	52
4.3.2 Flow Velocities – 100-Year	54
4.4 DTM Resolution Effect on Hydraulic Modeling	56

5.0 DISCUSSION	59
5.1 Introduction.....	59
5.2 Pre- to Post-Project Comparisons	60
5.2.1 Inundation Area	61
5.2.2 Flow Velocities	62
5.3 Ecological Importance	63
5.3.1 Salmon Populations	64
5.3.2 Changes in Peak Flood Occurrence	66
5.3.3 Ecological Interaction	68
5.4 DTM Resolution Effect.....	69
5.5 Cost Benefit	71
5.6 Future Research	72
6.0 CONCLUSION.....	74
REFERENCES	76
APPENDICES	81

List of Figures

Figure 1.1. Location of Greenwater River Floodplain Restoration	5
Figure 2.1. Oblique view of the three-dimensional lidar point cloud of all laser returns, 2007 Greenwater restoration area	18
Figure 3.1. Photos of 2017 lidar drone flight.....	25
Figure 3.2. Pre- and post-project lidar terrain used for hydraulic modeling.....	27
Figure 3.3. Greenwater basin drainage areas	29
Figure 3.4. 2017 Aerial imagery	32
Figure 3.5. National Land Cover Dataset within the Greenwater project area	33
Figure 3.6. Sample of data used to delineate Manning’s n roughness values.....	35
Figure 3.7. Depiction of combined structured and unstructured computational mesh. Breakline along FR 70 road surface is in red.	38
Figure 3.8. Example of cell and cell face detailed hydraulic tables (Brunner, 2016).....	39
Figure 4.1. Engineered log jam locations shown on the post-project bankfull inundation.....	42
Figure 4.2. Inundation areas for all flood events	44
Figure 4.3. Mean annual minimum inundation areas pre- and post-project	45
Figure 4.4. 1.6-year bankfull inundation areas pre- and post-project	46
Figure 4.5. 5-year inundation areas pre- and post-project	47
Figure 4.6. 10-year inundation areas pre- and post-project	48
Figure 4.7. 25-year inundation areas pre- and post-project	49
Figure 4.8. 50-year inundation areas pre- and post-project	50
Figure 4.9. 100-year inundation areas pre- and post-project	51
Figure 4.10. 10-year velocities pre- and post-project	53
Figure 4.11. 100-year velocities pre- and post-project	55

Figure 4.12. 100-year inundation areas on post project 1-foot and 3-foot gridded terrain	56
Figure 4.13. Mean annual minimum inundation areas on post-project 1-foot and 3-foot gridded terrain.....	58
Figure 5.1. StreamNet fish distributions by species	65
Figure 5.2. Annual peak streamflow 1912–2017 (top), Streamflow 2008–2017 (middle), Annual peak flow events > 10-year flood per decade (bottom)	67
Figure 5.3. Relationship between peak flow events and salmon life histories in the Greenwater River.....	69

List of Tables

Table 3.1. Drainage areas and peak flood levels.....	30
Table 4.1. 10-year velocities pre- to post-project	52
Table 4.2. 100-year velocities pre- to post-project	54
Table 4.3. Inundation areas on post-project 1-foot and 3-foot gridded terrain	57
Table 4.4. Mean velocities on post-project 1-foot and 3-foot gridded terrain	58
Table 5.1. Lidar cost comparison.....	72

Acronyms

cfs: cubic feet per second

DNR: Department of Natural Resources

DEM: digital elevation model

DSM: digital surface models

DTM: digital terrain model

ESU: evolutionarily significant unit

ESA: Endangered Species Act

ELJ: engineered log jam

FIPS: Federal Information Processing Standard

FR 70: Forest Road 70

GFDL: Geophysical Fluid Dynamics Laboratory

HEC-RAS: Hydrologic Engineering Center's River Analysis System

HECI: Herrera Environmental Consultants, Inc.

LWD: large woody debris

NAIP: National Agriculture Imagery Program

NIR: near-infrared

NAD83: North American Datum (1983)

NAD88: North American Vertical Datum (1988)

NLCD: National Land Cover Database

NOAA: National Oceanic and Atmospheric Administration

RCO: Recreation and Conservation Office

SPSSEG: South Puget Sound Salmon Enhancement Group

TIN: Triangulated Irregular Network

UAV: unmanned aerial vehicle

USGS: U.S. Geological Survey

WDFW: Washington Department of Fish and Wildlife

WSDOT: Washington State Department of Transportation

WRIA: Watershed Resource Inventory Areas

Acknowledgements

I would most like to thank my wife Shawna, who has supported me through the many years of transitioning my career back to that which I had always imagined for myself, working towards a goal of restoring and conserving our natural world. I would like to thank my three children, Nora, Jonas, and Ula, who gave up a bit of their dad to this transition, and who, along with all of my family and friends are as excited as I am for the completion of this thesis and my MES. I would also like to thank the team at the South Puget Sound Salmon Enhancement Group for all of their knowledge and support through my master's work, as well as the opportunity to continue this work professionally. Finally, I would like to thank my thesis reader, Ted Whitesell, for all of his guidance and patience with me throughout the writing process.

1.0 INTRODUCTION

Rivers and streams in the Pacific Northwest have been home to Pacific salmon species for over 6 million years (Waples, Pess, & Beechie, 2008). These salmon play an important role as a keystone species within the aquatic ecosystem that they are part of and the terrestrial riparian ecosystem that they move through. In the past century overharvesting and anthropogenic changes to the landscape, resulting in separation from and degradation of habitat, have led to the elimination of Pacific salmon across 40% of their historic range and reduced returns to 6-7% of their historic numbers (Gresh, Lichatowich, & Schoonmaker, 2000). Dams, culverts, and levees block rivers and change flow patterns, logging and other forms of deforestation have removed thermal protection and food sources, and agricultural and urban stormwater runoff is polluting waters that are detrimental to the survival of native salmon populations. In response, 6 salmonid species, which include 18 evolutionarily significant units (ESU), have been listed under the Endangered Species Act (ESA) in Washington State since 1991 (RCO, 2009). Recovering salmon populations through restoration to increase the health and natural function of our aquatic systems is a unifying goal across many government, tribal, and nonprofit entities. To accomplish this over a billion dollars is spent annually on river restoration projects in the US and it is a large focus for environmental management and policy decisions (Bernhardt et al., 2005).

With so much spent on salmon restoration, it is important to monitor the efficacy of these projects to ensure that we adapt our management practices to be most effective. These efforts not only help support fish and river systems but increase the ecosystem services we get from these precious resources. From clean water and flood resilience to

fishing and recreation, it is imperative that we continue revitalizing and restoring our natural waterways. In managing this work, it is also important to take into account the trends of a shifting climate.

Climate models show a distinct shift to warming temperatures caused by anthropogenic influences increasing greenhouse gases and changing the global carbon cycle, and recent global levels have already surpassed all other climate anomalies over the past 1500 years (Mann et al., 2009). When linking models of future climate, land cover, hydrology, and salmon populations, a large negative impact is seen to occur in freshwater salmon habitat and river basins that are fed by the current snowline, and salmon populations in these basins become especially vulnerable as they are faced with higher winter flows and lower summer flows (Battin et al., 2007; Mantua, Tohver, & Hamlet, 2010). Salmon have adapted and survived many fluctuations in global climate throughout their existence, but current levels of anthropogenic climate change are occurring at a much faster rate than the natural global climate cycles, and natural adaptations will likely not be able to keep up with the current rate of change. These changes are happening now, and we have already begun to see the results of a shifting climate, further highlighting the need for increased understanding of the efficacy of our restoration efforts.

Many methods have been developed to monitor the effectiveness of stream restoration. Primarily these involve on the ground surveys, but remote sensing and computer models have the potential to capture and predict the results of restoration, and may be able provide valuable information when constraints on time, budget or access prevent ground surveys and monitoring. As well, ground surveys can only capture the

conditions that exist on that day, while models—although not perfect—can provide a snapshot of multiple theoretical conditions.

The goal of this thesis is to examine how new advancements in drone based lidar and modeling technology can be utilized to quantify and visualize the results of stream restoration efforts, particularly how well the Greenwater River Floodplain Restoration Project, located north of Mount Rainier in Washington State, was able to achieve project goals, with a focus on the reconnection of the floodplain and seasonal side channels in order to reduce high flow velocities and increase flood resiliency by inserting woody debris and spreading flow out across the floodplain. To accomplish this, a 2D hydraulic model, which predicts two-dimensional, multi-directional flow across a three-dimensional terrain, was utilized to compare the area of inundation of the floodplain and the flow velocities at various flood stages before and after restoration. Topographic data for the hydraulic model were acquired from lidar datasets, incorporating a pulsed laser and receiver to measure distance and ultimately create a three-dimensional model of the target area, flown both pre- and post-project. The post-project lidar acquisition was collected by an unmanned aerial vehicle (UAV), more commonly known as a drone, which can provide very high-resolution topographical data for analysis. Possible benefits and uses of this higher resolution data are an additional goal explored in this research. Project changes to the landscape in the Greenwater River restoration were found to be successful in meeting project goals, and UAV lidar was found to provide a more cost-effective option, yielding a more detailed terrain model, useful not only in modeling floodplain inundation and flow velocities, but with the potential to provide insights into vegetation cover and instream habitat as well.

The project area of the Greenwater River was identified and funded for restoration primarily due to anthropogenic modifications to the landscape that separated the river from its flood plain and degraded salmon habitat. The project area is located along the border of Pierce and King Counties in the Mt Baker-Snoqualmie National Forest, Washington, and is a tributary to the White River, which feeds into the Puyallup River before emptying into the Puget Sound. See Figure 1.1. Historically the Greenwater Watershed supported healthy populations of fish, and was one of the essential spawning areas in the White River watershed for threatened Spring Chinook (Laurie, 2002). In the 1960s, clear-cut logging activities around the Greenwater River removed all but some small stands of trees close to the river. In December of 1977, a rain-on-snow event generated a record peak flow of 10,500 cubic feet per second (cfs). The flood flushed large logs, landslide debris and remnant logging material downstream, with much debris racking up on the Highway 410 Bridge, leading to record flooding in the town of Greenwater. By 1979, reactions to the flooding led managers to remove all woody debris from the river greater than 3-inches in diameter and 3-feet in length. The lack of riparian forests and instream wood led to a decrease in fish habitat caused by increased water velocities and shear stresses scouring the river bed, resulting in an incised main channel further removed from its floodplain. Restoration of the Greenwater River would be focused on improving aquatic and riparian habitat for currently threatened populations of Spring Chinook (*O. tshawytscha*) and steelhead (*O. mykiss*) utilizing the project area alongside Coho Salmon (*O. kisutch*) (Abbe, Beason, & Bunn, 2007; Ecology, 1998; Marks et al., 2016). Restoration efforts within the project area were performed between 2010 and 2014.



Figure 1.1. Location of Greenwater River Floodplain Restoration

The Greenwater River restoration project involved a number of restoration activities including large woody debris (LWD) placement in the form of 17 engineered log jams (ELJ), the removal of an abandoned forest road posing a barrier between the river and its floodplain, and riparian plantings. Successful restoration would increase floodplain connectivity and off-channel habitat. ELJs provide increased roughness, promote activation of relic side channels, encourage natural wood and sediment recruitment, and increase pool frequency—all with the goal of improving salmon habitat (Abbe et al., 2007; Cramer et al., 2012). Riparian plantings provide habitat complexity and future thermal protection. In monitoring the results of this and other projects,

decision makers should be able to use that knowledge to help identify the best restoration methods to use and the most beneficial areas to concentrate efforts.

This thesis first provides a review of the applicable literature. It then outlines research methods before providing model results. Next, a discussion of the results and their relevance is provided, followed by a conclusion of the findings. The literature review first examines the efficacy of stream restoration projects and the need for monitoring in order to be able to best adapt our practices to be most effective. It then provides a more in-depth look at how climate change is affecting salmon populations in the Pacific Northwest to illustrate the need for successful restoration to add resiliency to salmon-bearing streams and rivers. Finally, previous research on methods and the use of lidar-derived topographic models within a 2D hydraulic model is explored.

The methods chapter first provides additional details on the Greenwater River study area. It then outlines the data used to drive the hydraulic model, including lidar, flood discharge levels, and roughness values. Finally, specific model parameters are discussed followed by a description of the methods of analysis. Results are then presented, providing a quantified description of inundation area for various flood events comparing pre- and post-project condition results. This is followed by modeled flow velocities across the floodplain and within the spawning channel at the 10 and 100-year events. Inundation results are then compared on the post-project terrain for the native 1-foot resolution compared to the same terrain downsampled to a 3-foot grid cell.

The discussion chapter first considers the pre- to post-project comparisons of inundation and flow velocities, highlighting the specific improvements accomplished by the Greenwater River restoration. It then looks at specific fish life histories within the

Greenwater River and how those relate to recent increases in peak flood occurrences, attributed to climate change. This presents a direct correlation between high flow events and fish presence, showing the importance of this and other similar projects to reduce flow velocities for incubating and rearing fish. The small effect of the studied terrain resolution difference on model results is then discussed followed by the cost benefit of UAV to conventional lidar for the Greenwater River restoration and other projects covering a few 100 acres or less. Lastly, recommendations to improve future research are explored, including use of the UAV lidar point cloud to determine detailed roughness values, along with the capture of blue-green bathymetric lidar, to provide insight into fine-scale habitat features generally captured through on the ground, instream surveys.

2.0 LITERATURE REVIEW

2.1 Introduction

In this thesis 2D hydraulic modeling is used to analyze how well the Greenwater River Floodplain Restoration Project met projected goals related to floodplain and side channel activation, and the reduction of flow velocities. This contributes to the general knowledge regarding similar restoration efforts, as well as giving specific insight into the gains of this and future restoration plans in the Greenwater Basin. The use of a lidar-derived digital terrain model (DTM) as the primary input into the hydraulic model has been utilized in many previous studies to assess restoration efforts or flood risk (Herrera Environmental Consultants, Inc., 2010; Khattak et al., 2016; Quiroga, Kure, Udo, & Mano, 2016; Yang, Townsend, & Daneshfar, 2006). Recent advancements in drone and lidar technology are able to provide more detailed models of terrain than previously available. The possible benefits of UAV lidar for both cost effectiveness and providing a more precise terrain for use in hydraulic models and other analysis are also examined to provide restoration practitioners with information on the advantages and uses of this relatively new method of obtaining a very detailed DTM. Trends of a shifting climate causing changes in discharge patterns are also analyzed to highlight the need for restoration in the face of climate change.

Past studies were identified to give a better understanding of the need for monitoring restoration projects, as well as the uses and capabilities of hydraulic models. This chapter reviews the general effectiveness of restoration projects leading to the need for monitoring, the impacts of climate change on Washington salmon, and describes

techniques and uses of lidar in 2D hydraulic modeling, all providing a framework of how this research fits into the current knowledge base.

2.2 Monitoring the Effectiveness of Stream Restoration

In the late 20th century, the need to further improve salmon recovery efforts became evident. Thorough monitoring and analysis of the results of stream habitat restoration methods was not occurring, and their effectiveness was highly debated by the scientific community (Reeves et al., 1997). As we move further into the 21st century, most projects are still either not monitored or are poorly monitored (Bernhardt et al., 2005; O’Neal, Roni, Crawford, Ritchie, & Shelly, 2016). By monitoring the outcomes of restoration projects, management practices can be adapted to give the most desired results based on scientific evaluation. New methods and tools continue to be developed that can help practitioners in their monitoring efforts. This information can be used to plan future projects and set meaningful project goals, which should increase success and maximize effectiveness. Prior monitoring of restoration projects with similar aspects as the Greenwater restoration gives some insight into the expected results of restoration.

O’Neal et al. (2016) statistically assessed the success and effectiveness of 65 projects in the Pacific Northwest, across multiple project categories including fish passage, instream habitat, riparian planting, and floodplain enhancement. Elements of the Greenwater River Floodplain Restoration Project included floodplain enhancement and instream habitat improvement, through the use of ELJ placements, topographic modifications, and riparian plantings. Although this thesis investigates metrics not specifically addressed by O’Neal et al. (2016), the likely benefits of the Greenwater restoration are identified. In the O’Neal et al. (2016) study, the timeline of post-project

monitoring was estimated based on how much time a given restoration category would need to produce detectable results. For example, fish passage barrier removal projects were expected to show an impact soon after implementation so they were monitored at 1, 2, and 5 years after completion. Habitat projects such as LWD installations were expected to take longer before results could be seen and monitoring was scheduled to occur at 1, 3, 5, and 10 years after implementation. This research on the Greenwater River represents a 3-5 year post-project evaluation.

Instream habitat projects involving the placement of structures, such as ELJs, generally show improvements in the habitat indicators being assessed such as pool area, depth, sediment and wood volumes. In the O'Neal et al. (2016) study, the biologic response of fish numbers reported a general negative trend with juvenile Chinook and Coho Salmon being slightly negative but insignificant, and steelhead showing a significant negative trend in relation to placement of instream structures. Along with showing positive habitat indicators, structure placement is seen as successful when after the fifth year 90% of the structures are still in place, which is still the case for the Greenwater restoration. The lack of improvement in fish numbers, along with some negative responses, could be because salmonid populations need longer to respond, adapt, and recover from changing habitat conditions. Similar negative fish responses have been noted in other studies (Stewart, Bayliss, Showler, Sutherland, & Pulin, 2009; Whiteway, Biron, Zimmermann, Venter, & Grant, 2010). This may also be pointing to the possibility of limiting factors that should be addressed elsewhere in the system, causing a general negative trend in fish populations throughout the watershed. Even though the effect of these structures on fish populations has not been positively correlated, resulting

improvements to habitat features continue to foster the popularity of instream structure projects.

Floodplain enhancement projects have been found to increase the bank-full width, flood-prone width and mean canopy density. Fish densities assessed for these projects were fairly low across most of the sites assessed, with some increases in Coho Salmon densities. Off-channel habitat found in floodplains is thought to provide a velocity refuge for juvenile fish (Beechie, Liermann, Pollock, Baker, & Davies, 2006). The benefits of floodplain enhancement and connectivity projects may also be able to minimize the scouring effects of high flows during periods of flooding (O’Neal et al., 2016).

Riparian planting projects assessed show an increase in woody species cover and exceeded plant survival criteria. The percent canopy cover did not change in the 5 years of monitoring done by O’Neal et al. (2016) and will most likely need significantly more time to show an increase. As well, no differences were noted in a reduction of active bank erosion after 5 years and will likely also require more time to see results. Because riparian planting projects require a longer timescale, fish densities were not looked at for those projects. Riparian plantings have been shown to be ecologically beneficial but are difficult to prove significant change due to the long timescale needed for planted vegetation to mature. Even though an immediate ecological response to these projects is not seen, they still provide a potential long-term benefit to future changes in flow and stream temperature that are likely to occur due to climate change.

Overall the study performed by O’Neal et al. (2016) showed that instream habitat, floodplain enhancements, and riparian plantings, which were all part of the Greenwater restoration, led to significant improvements in physical habitat after 5 years, even though

increased fish densities did not necessarily correlate with these projects. These results give us some insight into the effectiveness of these projects to meet goals of increasing the overall ecological and functional health of our waterways, but the biological response of salmonids to restoration is the primary factor that we are concerned with and is stated to be the “ultimate measure of restoration effectiveness” (O’Neal et al., 2016). Due to the large variability in the interannual abundance of salmonids, monitoring for 10 years or more is recommended to truly observe the effectiveness of restoration (Bisson, Quinn, Reeves, & Gregory, 1992; Reeves et al., 1997). As we plan for future projects, we should consider these results along with our knowledge of salmon life histories and the ecology of the rivers in which they incubate, rear, migrate through, and hopefully return to spawn in. Continuing to hone and develop monitoring methods along with growing the database of results should provide the tools needed to be most effective in adapting our management of streams and river. This becomes especially important in order to increase resilience of fish-bearing streams to a future, unknown climate.

2.3 Climate Change and Salmon

In the past century, human activities including overfishing and changes to the landscape have led to reduced, threatened and endangered salmon populations. Many goals of restoration target historic conditions at a time before modern human disturbances. However, changes in our global climate that are predicted to occur in the relatively near future may dramatically change how rivers function, and managers should consider more than just restoring rivers to their historic state. Land use shifts and unprecedented climate change are also leading to changes in biodiversity that can make the goal of restoring to a past environment unrealistic and ineffective (Choi, 2007).

Hence, we must consider more “forward-looking” paradigms that include enhancing ecosystem services and increasing resilience in the face of future climate change (Suding, 2011). This may be accomplished by focusing on the abundance of target species relative to project areas, the composition of native species, and healthy ecological processes (Thorpe & Stanley, 2011).

Shifting climates within the greater Pacific Northwest and specifically the Greenwater River basin are following trends predicted by future climate models. The Northwestern U.S. has warmed between 0.7° to 0.9° Celsius (C) during just the 20th century, in contrast to the 1° C in warming over the previous millennium, and climate models predict another 1.5° to 3.2° C in warming by the middle of the 21st century (Mann et al., 2009). Results modeled by Battin et al. (2007) in the Snohomish River Basin led to consistently negative impacts on freshwater salmon habitat, including higher water temperatures, lower spawning flows, and increased winter peak flows. These models predict a decline of Chinook salmon populations by 20-40% by 2050 in the absence of further habitat restoration, with the greatest effect being seen during spawning and incubation periods in the high-elevation areas, due to the impact on egg survival by increased peak flows. This predicted negative effect of climate change may be conservative as they did not model the impact of sea level rise and ocean warming that will likely also decrease the salmon’s survival. When associating Geophysical Fluid Dynamics Laboratory’s (GFDL) R30 climate model results with restoration plans, it was shown that by completing a full suite of restoration efforts we could limit the population declines to 5% with a possibility of increasing salmon abundance when using the Hadley Center’s HadCM3 model (Battin et al., 2007).

A study by Mantua et al. (2010) assessed the hydrologic changes in watersheds across Washington State, and how predicted changes would affect the reproductive success of salmon. Averages based on 19 scenarios predicted increases in annual temperature in the Pacific Northwest compared to the 1980s to be 1.2° C by the 2020s, 1.9° C by the 2040s, and 3.2° C by the 2080s. Averaged annual precipitation change was small, but models predicted large seasonal changes towards wetter winters and drier summers. Hydrologic modeling showed a complete loss of snowmelt dominant basins across Washington by the 2080s, with only 10 basins in the North Cascades remaining as transient basins, fed by a mix of rain and some snow. Many of Washington's current transient runoff basins, including the Greenwater River Basin, are predicted to be fed primarily by rainfall, which will lead to a dramatically increased magnitude and frequency of flooding in the months of December and January (Mantua et al., 2010).

Mantua et al. (2010) lists the effects on salmon as follows. Significant stream temperature increases will lead to thermal stress for all salmon that have a life history that puts them in freshwater during summer for spawning, rearing, or smolt migrations. This will be most severe for salmon populations that have summertime migrations that rely on thermal cues to initiate spawning migration. As well, the loss of adequate rearing habitat caused by increased stream temperatures will negatively affect both summer and winter runs of stream-type Chinook, Coho Salmon, and steelhead, which spend at least one summer—typically two for steelhead—rearing in freshwater streams. The movement away from snowfall to rain, increasing the magnitude of winter flooding, will have a varying impact across species, depending on the depth of the gravel spawning nests, or redds, they create. Deeper redds, generally made by bigger fish, will be less vulnerable in

these conditions. A lack of snowmelt will also affect smolt migrations that have evolved to match the timing of cooler, snow-fed flows. Changes in these thermal timing events could also lead to a mismatch with the ocean prey and/or predator fields. Cool season stream temperature changes were not assessed by Mantua et al. (2010), but it is noted that warming in winter and spring could lead to earlier and longer growing seasons, increasing the aquatic food-web productivity, which could aid in more rapid juvenile salmon development rates (Schindler & Rogers, 2009). Considering all the impacts of a changing global climate on salmon, the resilience of restoration projects becomes even more important.

These modeled effects of climate change all point to recovery targets becoming increasingly difficult to meet, as environmental stress on salmon populations increases (Battin et al., 2007). Ecological resilience will be key to ensuring that restoration is sustainable and will not require intensive and ongoing intervention in the face of environmental change (Suding, 2011). The Greenwater restoration has incorporated methods that add increased resilience to the basin by reducing high flow velocities and increasing thermal refuge habitat through LWD placement. Post-project lidar input into a hydraulic model allow for the quantification of many of the benefits gained by the Greenwater restoration and other stream restoration projects.

2.4 Hydraulic Modeling Using Lidar

One method of monitoring the effectiveness of wood placement and floodplain reconnection projects is through the use of hydraulic models. If adequate topographic data are available, from cross-sections or lidar bare-earth models, a hydraulic model can be developed to examine water flow and floodplain attributes such as inundation and

velocity. These attributes are especially important to spawning and rearing salmonid populations (Jeffres, Opperman, & Moyle, 2008). The results from the hydraulic model can help us set meaningful goals pre-project and check the efficacy of the completed restoration project to meet those goals.

There are a number of hydraulic modeling software packages available today. Terrain data input into these models are generally 1D, 2D, or a combination of the two. Modeling in 1D solves one-dimensional equations of flow using a sequence of cross-sections connected by an interpolated surface on which flow is modeled. One-dimensional models are a more simplified representation of reality (Costabile, Macchione, Natale, & Petaccia, 2015). When modeling in 1D, flow is solved only in one dimension, perpendicular to the cross-sections. Hence, 1D modeling only provides a single water level, velocity and flow rate for each cross-section in the model, while 2D modeling may show significant variability across the same section. If there are enough cross-sections available, the 1D model can provide a good representation of the topography of the riverbed. One-dimensional models also have the advantage of running computations relatively quickly. One-dimensional models, however, are limited by the interval between cross-sections and their extent into the floodplain. They also require a time investment in gathering enough cross-sections to accurately describe the channel. One-dimensional modeling can be useful to identify detailed descriptions of flow through the channel, but can find greater use when combined with 2D modeling (Brunner, 2016).

Two-dimensional flood modeling solves for 2D equations of flow, allowing for flow in any direction across the terrain surface from higher to lower areas. The terrain input into a 2D model is generally in the form of a DTM, which provides a three-

dimensional topographic surface of the entire floodplain. This type of modeling calculates flow routes, velocity and depth distribution across the floodplain. Two-dimensional models can be computationally slower, but are more useful when a detailed description of the floodplain is required.

Data input into the 2D hydraulic model primarily include terrain data, a stream discharge hydrograph, and roughness. The terrain is generally captured using lidar (light detection and ranging) technology. Discharge is available from various USGS stream gages, and roughness is discussed later in this section. Lidar is a remote sensing method in which the combination of a pulsed laser, receiving scanner, and highly accurate GPS receiver are used to accurately measure distances, resulting in a three-dimensional model of the target environment. Lidar data are output in a point cloud of laser returns, which is then converted into a Triangulated Irregular Network (TIN) or raster DEM. See Figure 2.1 for a two-dimensional representation of the three-dimensional lidar point cloud.

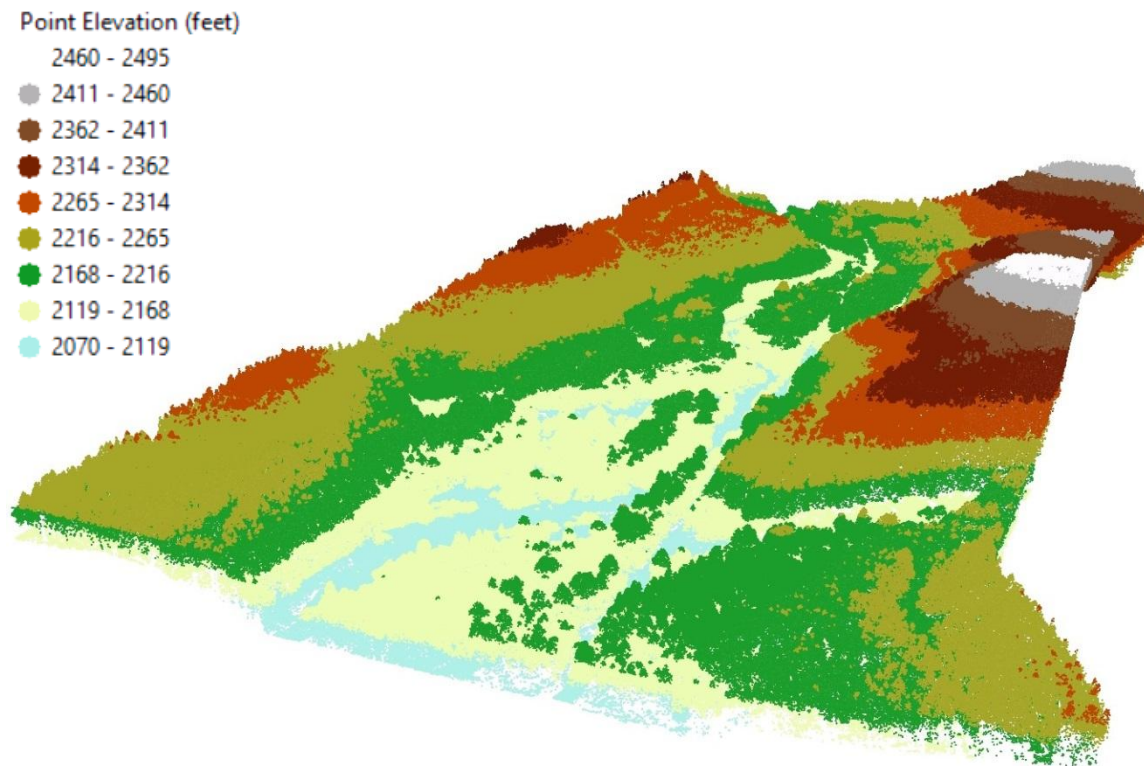


Figure 2.1. Oblique view of the three-dimensional lidar point cloud of all laser returns, 2007 Greenwater restoration area

When there is a need to use previously captured topographic data you are limited by what is available in your study area. As technology has advanced, the resolutions of available topographic data have increased over the years. The effect of topographic grid sizes on hydraulic model outputs should be considered. It has been noted that a higher resolution terrain does not necessarily output higher quality results (Charrie & Li, 2012; Costabile et al., 2015). In the study performed by Charrier & Li (2012) a 1-meter lidar digital elevation model (DEM) was downsampled to 3, 5, 10, 15, and 30 meters, and hydraulic model outputs were compared. The 3-, 5-, and 10-meter DEMs produced similar results, within 2%, 3.6%, and 2.8% respectively, to the 1-meter DEM. The 15- and 30-meter DEMs both resulted in a 6.8% difference from the target 1-meter DEM.

When floodplain inundation from the 1-meter DEM was compared to models run on USGS 5-, 10-, and 30-meter DEMs differences were -12.6%, -9.3%, and -1.2% respectively. This suggested that different data sources produced more significant changes in results than downsampling a single data source. This thesis explores effects resulting from the next level of topographic resolution difference from 3-foot (approx. 1 meter) to 1-foot resolution. Besides providing the base terrain for the 2D hydraulic model, lidar outputs can be used to inform roughness values.

Lidar has been shown to be useful in stream and riparian habitat analysis and monitoring (Cavalli, Tarolli, Marchi, & Fontana, 2008; McKean, Isaak, & Wright, 2009). Various outputs can be produced from analysis of lidar in the GIS environment. Some of these outputs can be used in the development of accurate Manning's n roughness determinations. Roughness values reflect impedance to flow that occurs on and above the terrain surface, and can have a significant impact on modeled velocity, depth, and extent of inundation (Golshan, Jahanshahi, & Afzali, 2016). Vegetation plays a large part in the roughness of the floodplain, and vegetation heights derived from the difference between bare-earth and highest hit terrain models are useful in parameterizing roughness (Mason, Cobby, Horritt, & Bates, 2003; Quang Minh & La, 2011). Lidar intensity and aerial imagery are also useful in classifying roughness (Quang Minh & La, 2011). The methods listed above were the primary processes used in this thesis for determining roughness.

Another method of assigning roughness that was not incorporated in this study is through the inspection of the lidar point cloud. Research produced by Casas, Lane, Yu and Benito (2010) describes a method for parameterizing roughness by analyzing the sub-grid lidar data points above and below the bare-earth lidar surface. This method seems

very promising for describing highly detailed changes in roughness, and would be recommended when modeling to determine fine-scale habitat utilizing subsurface topography that can be acquired through bathymetric lidar.

2.5 Summary

The use of lidar within a 2D hydraulic model is seen to be a useful tool for assessing the outcomes of floodplain restoration projects. As we move into a more pronounced age of climate change, the need to assess these and other restoration projects in order to adapt and manage our goals and techniques is becoming even more important in the effort to slow and, hopefully, one day reverse declines in populations of Northwest salmon. As seen in other successful projects, the Greenwater restoration incorporates ELJs and topographical modifications, resulting in a reconnection of the floodplain and a subsequent reduction in flow velocities. Native plantings and LWD placements also lead to increased habitat and flood resilience. This research first assesses the effectiveness of the Greenwater River Floodplain Restoration Project. Second, it analyzes the use of UAV lidar. By monitoring this project as well as exploring the benefits of new drone based lidar technology utilized in this research, restoration practitioners should be able to make more informed decisions on when to incorporate these tools into future project monitoring and planning efforts.

3.0 METHODS

3.1 Introduction

One goal of this research is to model the hydrology of the Greenwater River as it flows through the Greenwater River Floodplain Restoration Project area in an effort to analyze the effectiveness of restoration. Secondly, this research identifies the effects of a higher resolution DEM, captured via UAV-mounted lidar, on hydraulic model outputs. To attain the first goal, a comparison was made between pre- and post-project model results at various flood stages to investigate the change in floodplain and side channel connectivity and flow velocities within the channel. The results of this research roughly mirror the pre-project assessment performed by Herrera Environmental Consultants, Inc. (HECI) in 2010. This methodology was chosen so that a comparison to the pre-project assessment's projected outcomes could be made. Pre-project lidar data were collected in 2007. Post-project conditions were captured by lidar in late 2017.

Hydraulic modeling was done using the US Army Corps of Engineers Hydrologic Engineering Center's River Analysis System (HEC-RAS) software version 5.0.3. HEC-RAS was chosen for use in this research because it is a reputable 2D hydraulic model provided free of charge by the USGS (Golshan et al., 2016; Khattak et al., 2016). HEC-RAS was recently updated in February of 2016 to include 2D modeling capabilities, allowing for lidar data to be used as the primary terrain input into the hydraulic model. Results from the analysis as described in this thesis are reported to the South Puget Sound Salmon Enhancement Group (SPSSEG), Washington State Recreation and Conservation office (RCO), Puyallup Tribe, Muckleshoot Tribe, King County Flood Control District, Washington Department of Fish and Wildlife (WDFW), Forest Service, National Oceanic

and Atmospheric Administration (NOAA), Watershed Resource Inventory Areas (WRIA) 10/12 Salmon Recovery Lead Entity, and the Puyallup River Watershed Council.

In addition to determining the effectiveness of the Greenwater River Floodplain Restoration Project, this research also explores the possible benefits of high-resolution UAV lidar to improve the accuracy of hydraulic model outputs and other analysis, as well as for cost efficiency. Drones are able to fly much lower and slower over the terrain, capturing a denser laser return point cloud than typically achieved from lidar flown by conventional manned aircraft. Lidar flown with a UAV can thus yield a higher resolution terrain model as well as a more detailed representation of the vegetation and other features above the surface. As similarly done by Charrier & Li (2012), downsampling the 2017 lidar data for this research explores the effects of using various resolution terrain inputs on hydraulic model outputs and parameters. This also provides an understanding what amount of error might be presented in comparing the lower resolution pre-project to the higher resolution post-project terrain modeled results.

This chapter gives an overview of the study area, discusses model inputs, details the methods used to run the hydraulic model, and outlines the methods of analysis between different model runs. It also discusses how key decisions were made in the process.

3.2 Study Area

The study area comprises a 1.5-mile reach of the Greenwater River located in Washington State. See Figure 1.1. The Greenwater River is a fifth-order tributary to the White River located along the border of Pierce and King Counties in the Cascade

Mountains north of Mount Rainier. The entire restoration site is federal land, managed by the US Forest Service within the Mt. Baker-Snoqualmie National Forest. The Greenwater River is documented to support spawning and rearing salmonid species, including Spring Chinook, Coho Salmon, and steelhead (Abbe, Beason, & Bunn, 2007; Ecology, 1998; Marks et al., 2016). Snorkel surveys of the project reach in 2014 and 2016 observed rearing Coho Salmon and Chinook Salmon in pools and side channels, and Coho Salmon were observed to be spawning in the upper reaches of the project area (Brakensiek, 2017). The project reach has seen many negative effects to the riverine ecosystem due to past logging activities and the clearing of large wood from the river. In an effort to restore the ecological health of the river, the Greenwater River Floodplain Restoration Project was started in 2010 with the completion of Phase 3 in 2014. Primary aspects of the restoration project impacting this research were the construction of 17 engineered log jams and the removal of a section of Forest Road 70 (FR 70) that separated the river from part of its floodplain. Riparian plantings also contributed to roughness of the floodplain and provide future instream cover and habitat complexity.

3.3 Data

The primary data used to create the hydraulic model of pre-project conditions was a 2007 bare-earth digital elevation model. Additional data used to inform both pre- and post-project models incorporates river gage discharge, basin statistics, aerial imagery, landcover, and lidar highest hit digital surface models (DSM). The elevation models of post-project conditions were created using lidar flown in December, 2017. The Hydraulic Assessment of Restoration Alternatives: Greenwater River Engineered Logjam Project Report (HECI, 2010), which modeled 2007 lidar data using FLO-2D modeling software,

was used to verify HEC-RAS 2007 model inputs and results. The 2007 data were remodeled for this research so a more direct and accurate analysis could be made between the 2007 and 2017 model results. A detailed description of the data and sources is presented below.

3.3.1 Lidar

In order to determine the effectiveness of the Greenwater River restoration, a comparison is made between past and present conditions, represented primarily by elevation models from 2007 and 2017 lidar acquisitions. Watershed Sciences, Inc. collected 2007 lidar data between May 22-25 for the Washington State Department of Transportation (WSDOT) and the SPSSEG. Lidar was obtained utilizing a Leica ALS50 Phase II laser system mounted in a Cessna Caravan 208, acquiring >105,000 laser pulses per second. Lidar points were corrected with a root mean square error of 0.10 feet, a 1-sigma absolute deviation of 0.10 feet and a 2-sigma absolute deviation of 0.20 feet (Watershed Sciences, 2007). Both bare-earth and highest hit models were determined at 3-foot resolution. Data output used the Washington State Plane North Federal Information Processing Standard area (FIPS) 4601 coordinate system in the 1983 North American Datum/1988 North American Vertical Datum (NAD83/NAVD88), reported in US survey feet (Watershed Sciences, 2007). The data were downloaded for this project from the Washington Department of Natural Resources (DNR) lidar portal. Lidar from DNR was provided in GeoTIFF format, which could be imported directly into the hydraulic model as the primary terrain data.

Post-project lidar data were collected by Flight Evolved on December 7, 2017 for SPSSEG. Lidar was obtained utilizing a Riegl VUX-1 LR mounted on a DJI Matrice 600

Pro drone, with the ability to acquire 750,000 laser pulses per second. Lidar points were corrected with a root mean square error of 0.169 feet and a standard deviation of 0.206 feet. Both bare-earth and highest-hit models were determined at 1-foot resolution. It was hoped that a higher resolution DTM could be produced but, due to dense canopy in the project area limiting the amount of laser ground returns making it back to the lidar device, the point spacing of the bare-earth lidar point cloud would not accurately support raster resolutions finer than a 1-foot grid. Pictures taken of the 2017 lidar flight are shown in Figure 3.1.



Figure 3.1. Photos of 2017 lidar drone flight

Lidar flights in both 2007 and 2017 collected data using standard near-infrared (NIR) lidar. Blue-green lidar capable of capturing bathymetry, the terrain under the water surface, was not available for pre- or post-project conditions. Without bathymetry, the pool-riffle sequence and subsurface topographical features such as boulders, root wads and other obstructions that cause friction to water flow must be represented in equations that drive the hydraulic model through increased Manning's roughness values (Crowder & Diplas, 2000). This method can predict average depth and velocity, but is not able to identify exact flow patterns or fine-scale ecological features in the vicinity of these obstructions (Crowder & Diplas, 2000). Manning's n roughness values were originally tabulated according to numerous factors posing a resistance to flow by Chow (1959). In essence, results from hydraulic models using channel roughness to replace the absence of bathymetry data are adequate for reach-scale analysis of floodplain inundation and average velocities needed for this analysis, but would not provide accurate representation of fine-scale individual habitat features such as detailed pool/riffle sequences and their metrics, which are typically captured through instream surveys.

Discharge at the time of the lidar flights was at relatively low flows, allowing for some, but not all, in-channel features to be captured, and required appropriate roughness values to accurately model velocities through the wetted channel. Lidar from 2007, flown during slightly higher discharge than in 2017, and producing a lower resolution 3-foot grid cell DTM, masked more of the fine-scale topographical features than the higher resolution 2017 lidar data flown during lower discharge. The HECI (2010) hydraulic report was faced with the same limitations of the 2007 data. Inspection of the 2007 lidar data by HECI assessed that it provided a good representation of the topography of the

area and was appropriate for the level of detail needed for hydraulic modeling of local floodplain inundation and velocity. The 2017 lidar, flown during relatively low discharge should provide a more detailed description of topographical features within the channel. Various resolutions of the 2017 DTM were modeled to determine possible changes in these local flow patterns relative to terrain detail. As the size of the grid cell in the DTM is increased, subgrid level features are lost to an average smoothing of the terrain surface and variations in local flow patterns within the channel are expected to decrease. Pre- and post-project bare-earth lidar are shown in Figure 3.2.

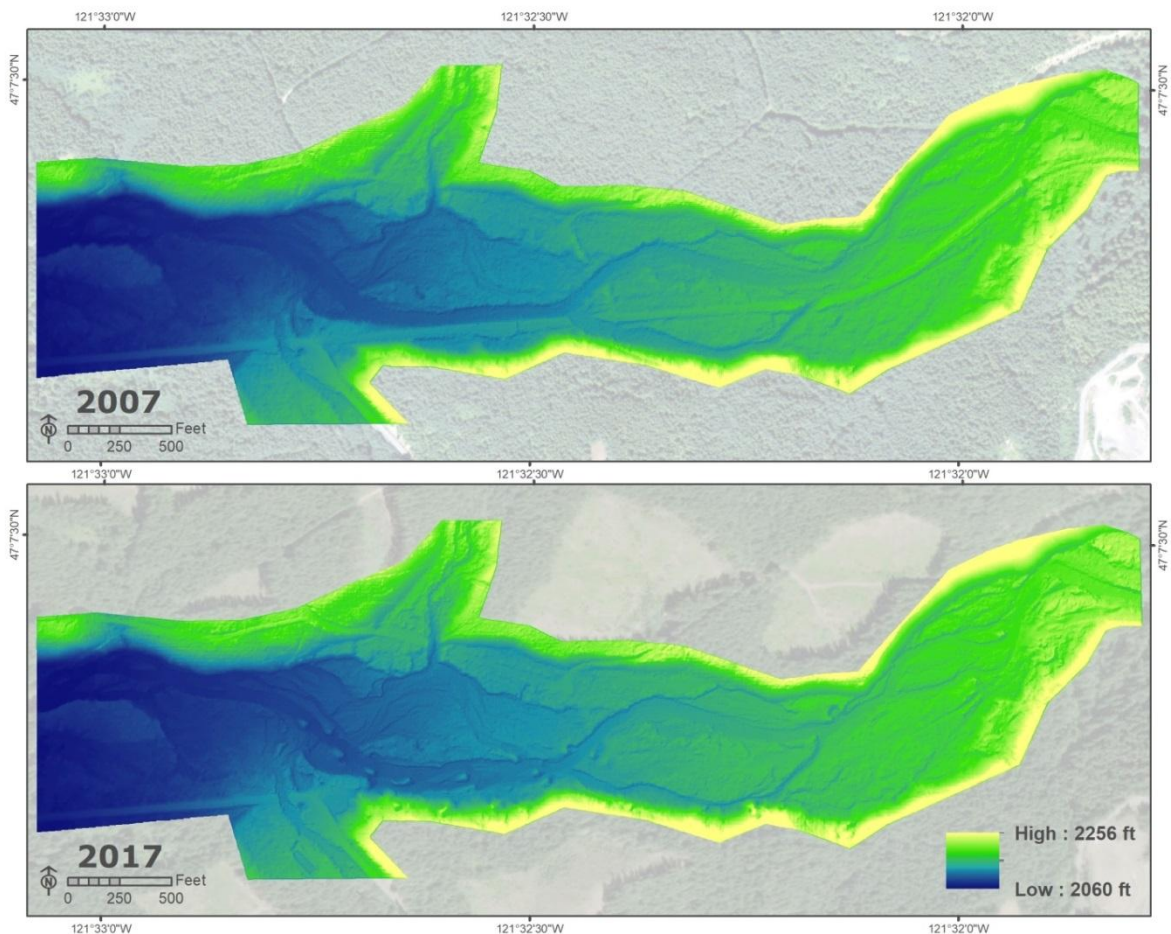


Figure 3.2. Pre- and post-project lidar terrain used for hydraulic modeling

3.3.2 Discharge and Basin Statistics

The U.S. Geological Survey (USGS) measures discharge flows at various gage locations and reports these data through the National Water Information System: Web Interface. USGS river gage station number 12097500, located on the Greenwater River at Greenwater, Washington, is the closest river gage to the project site, approximately 5 miles downstream. The highest peak flood flow was recorded in November 1977, at a discharge of 10,500 cfs. Gage daily mean discharge during the 2007 lidar flight window ranged from 303 to 338 cfs, with an average daily flow of 317 cfs over the 4 day acquisition period. This discharge is higher than the mean annual flow of 211 cfs, averaged over 70 years, but well below the bankfull flow of 871 cfs, representing the stage at which the water level tops the channel before it spills out into the floodplain (Laurie, 2002). Gage discharge during the 2017 lidar flight recorded at a daily mean discharge of 210 cfs.

The hydraulic model developed for this research required inflow discharge values at the upstream end of the project area and two tributaries. Because there is no USGS flow gage located within the project area, the discharge for the inflows into the model must be adjusted from the Greenwater River gage at Greenwater, Washington. Basin area characteristics were determined using data gathered from the USGS StreamStats web application, which delineates drainage areas for selected locations along stream lines. The required discharge inflows were determined using the ratio of basin drainage area at the gage to the basin areas at the inflow points to approximate discharge flow at the inlets for the various flood stages to be modeled. Basin areas are shown in Figure 3.3 and calculated discharge values are shown in Table 3.1. This method provides a reasonable

estimation when discharge is required at a location upstream of a stream gage. There is a margin of error in this method as it assumes the same contributing precipitation and groundwater upwelling across the whole area, and does not take into account snowmelt contributions primarily located in the upper watershed. Upon reviewing source discharge values used in the pre-project hydraulic assessment performed by HECI (2010), this discharge estimation method is observed to be the same method used to estimate previous modeled values.

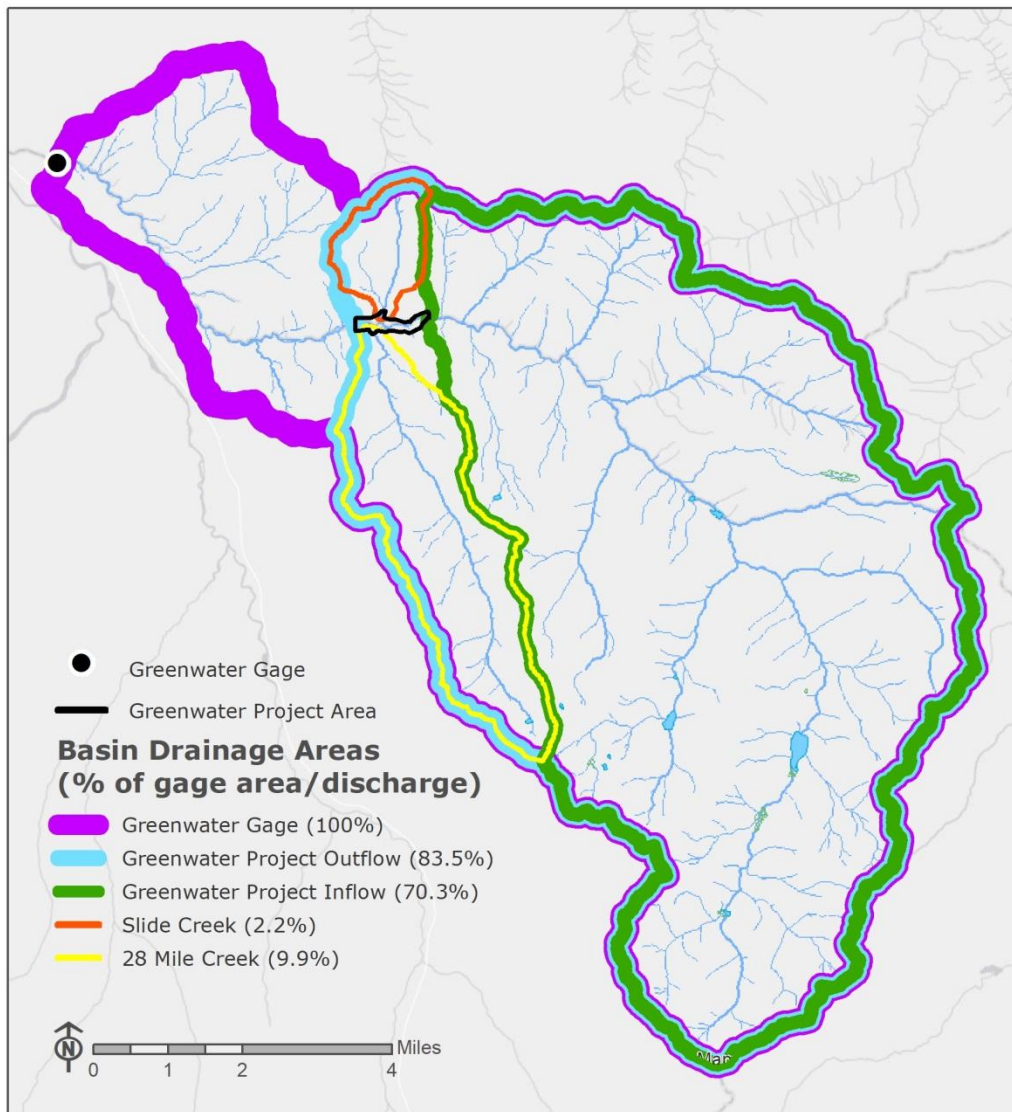


Figure 3.3. Greenwater basin drainage areas. Project area flow moves from east to west.

Table 3.1. Drainage areas and peak flood levels

Downstream Location of Calculated Drainage Area/Discharge	Drainage Area (square miles)	% of Gage Drainage Area / Discharge	Peak Flood Levels, 1911-2014 (cfs)									
			Mean Annual	Mean Annual Min	1-year	1.6-year	2-year	5-year	10-year	25-year	50-year	100-year
Greenwater Project <u>Outflow</u>	61.33	83.52%	77	176	274	877	1,203	2,163	3,007	4,335	5,537	6,949
Greenwater Project <u>Inflow</u>	51.60	70.27%	65	148	230	738	1,012	1,820	2,530	3,647	4,659	5,847
28 Mile Creek Confluence	7.30	9.94%	9	21	33	104	143	257	358	516	659	827
Slide Creek Confluence	1.61	2.19%	2	5	7	23	32	57	79	114	145	182
Project Reach (unnamed flow lines)*	0.82	1.12%	1	2	4	12	16	29	40	58	74	93
Greenwater <u>Model Inflow</u> **	52.42	71.39%	66	151	234	750	1,028	1,849	2,570	3,705	4,733	5,939
Greenwater Gage (No. 12097500)	73.43	100.00%	92	211	328	-	1,440	2,590	3,600	5,190	6,630	8,320
Greenwater Gage (No. 12097500) ***	100%	-	-	494	1,050	1,267	2,335	3,439	-	7,650	10,534	
Greenwater Project <u>Outflow</u> (Herrera Model <u>Inflow</u>)	83%	-	-	410	871	1,052	1,938	2,854	-	6,350	8,743	
***Peak Flood Levels, 1912-1996 (Abbe et al., 2007; HECI, 2010; Laurie, 2002)												

Greenwater Gage Values
HEC-RAS Model Inflow Values
Flow-2D Model Inflow Values (HECI, 2010)

* Project Reach = Project Outflow - (Project Inflow + 28 Mile Creek + Slide Creek)

** Greenwater Model Inflow = Project Inflow + Project Reach

It is important to note that models run by HECI (2010) used flood discharge values calculated through 1996, reported in Abbe et al. (2007), which were partially sourced from Laurie (2002). The analysis done for this research, using HEC-RAS, utilized the most current flood values posted by the USGS, determined through 2014, and adjusted for basin area. There is a significant difference between older peak flood levels using data through 1996 and current discharge values using data through 2014. This is most notable for the 100-year flood, which was reduced from 10,534 to 8,320 cfs—a difference of 2,214 cfs. Combined with computational and procedural differences between the two modeling software packages, this resulted in further variation in model results for specific flood levels run on the 2007 lidar data in HEC-RAS versus the previous model results run in FLO-2D, and should be considered when comparing results. Because there is no bankfull discharge values at the 1.6-year flood occurrence

using the current reported USGS discharge, the HEC-RAS model used the 1.6-year bankfull discharge reported by (Laurie, 2002). This value is considered acceptable as it falls within the range between the current 1- and 2-year discharges, and allows for a more direct comparison between the previous and current model runs on the 2007 terrain.

Another difference between the previous and current models is that previous models used Greenwater project area outflow values as the inflow at the top of the project, and did not model tributary inflows separately. There are two significant tributaries that flow into the Greenwater River within the project area. The current model used for this research applies discrete tributary flow inputs apart from the Greenwater model inflow applied to the top of the project reach. Greenwater River discharge flow values for the top of the project in the HEC-RAS model are based on accumulation from the basin above the project along with local surface accumulation above the outflow point not captured in the tributaries of Slide Creek and 28 Mile Creek. This local surface accumulation is referred to as Project Reach (unnamed flow lines) in Table 3.1, accounting for 0.82 square miles of area.

3.3.3 Aerial Imagery

Pre-project aerial imagery was gathered from the National Agriculture Imagery Program (NAIP). Imagery was not available for 2007 so data from 2006 and 2009 were acquired. Both 2006 and 2009 imagery showed no visible clearing or logging activity and appeared virtually identical outside of the time of day the image was acquired. Both images were considered to be a good representation of 2007 conditions. High-resolution aerial imagery was collected by drone photography on the same day as the 2017 lidar

flight, with a resolution of 3-inch grid cells. Samples of the 2017 aerial imagery are shown in Figure 3.4. Locations of ELJs are highlighted in the top two images.

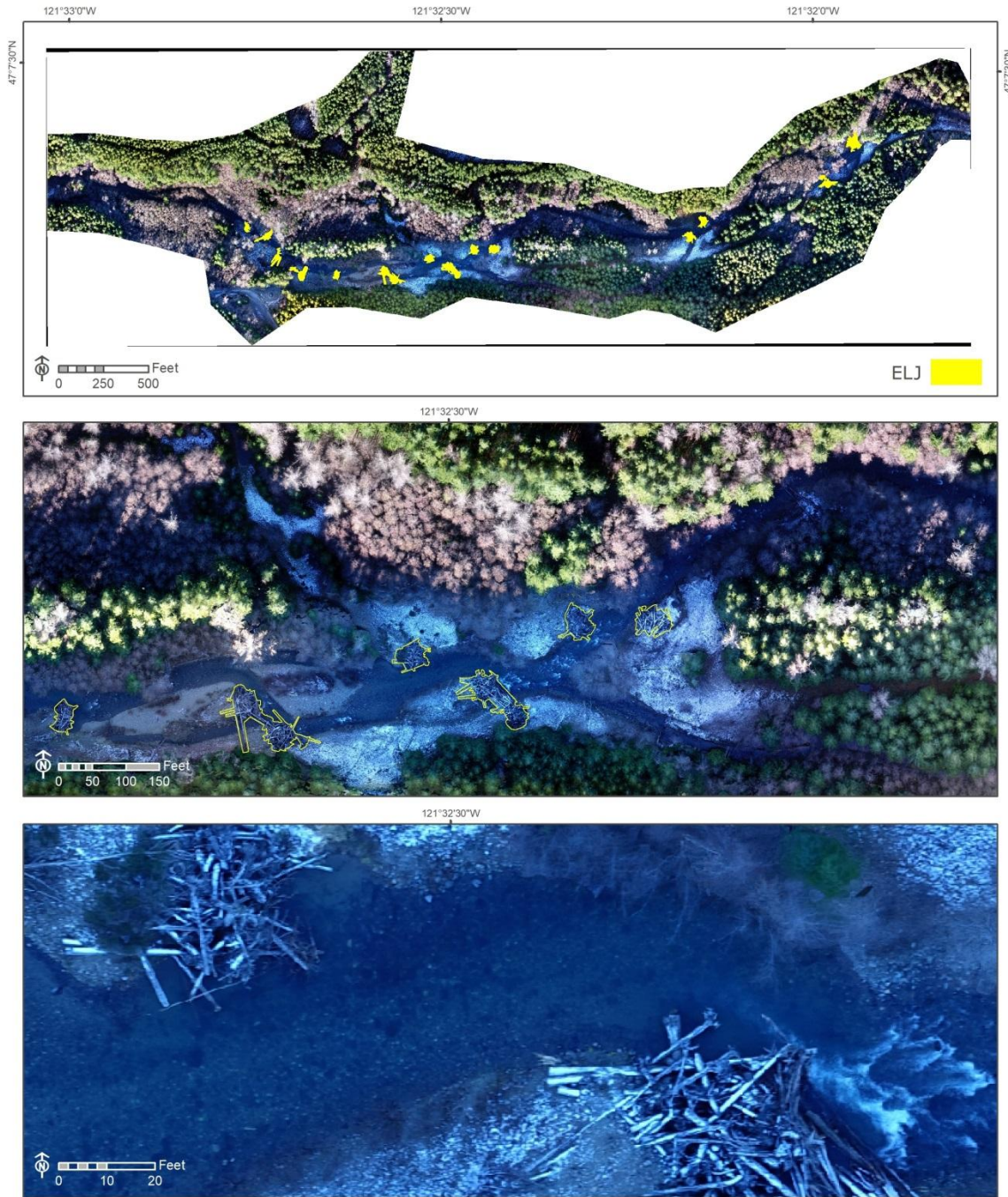


Figure 3.4. 2017 Aerial imagery

3.3.4 Land Cover and Manning's n Roughness Values

An accurate representation of land cover in the form of Manning's n roughness values is used in model calculations to parameterize the surface friction effects on water flow. Existing land cover datasets are typically used to assign roughness values (Brunner, 2016). Upon inspection of the National Land Cover Database (NLCD) in the project area, both accuracy and precision of the dataset were determined to be spatially unreliable and at an unusable scale to inform roughness values for the hydraulic model. As seen in Figure 3.5, resolution of the data is very low and depicts areas that do not accurately align with ground features such as the road and river.

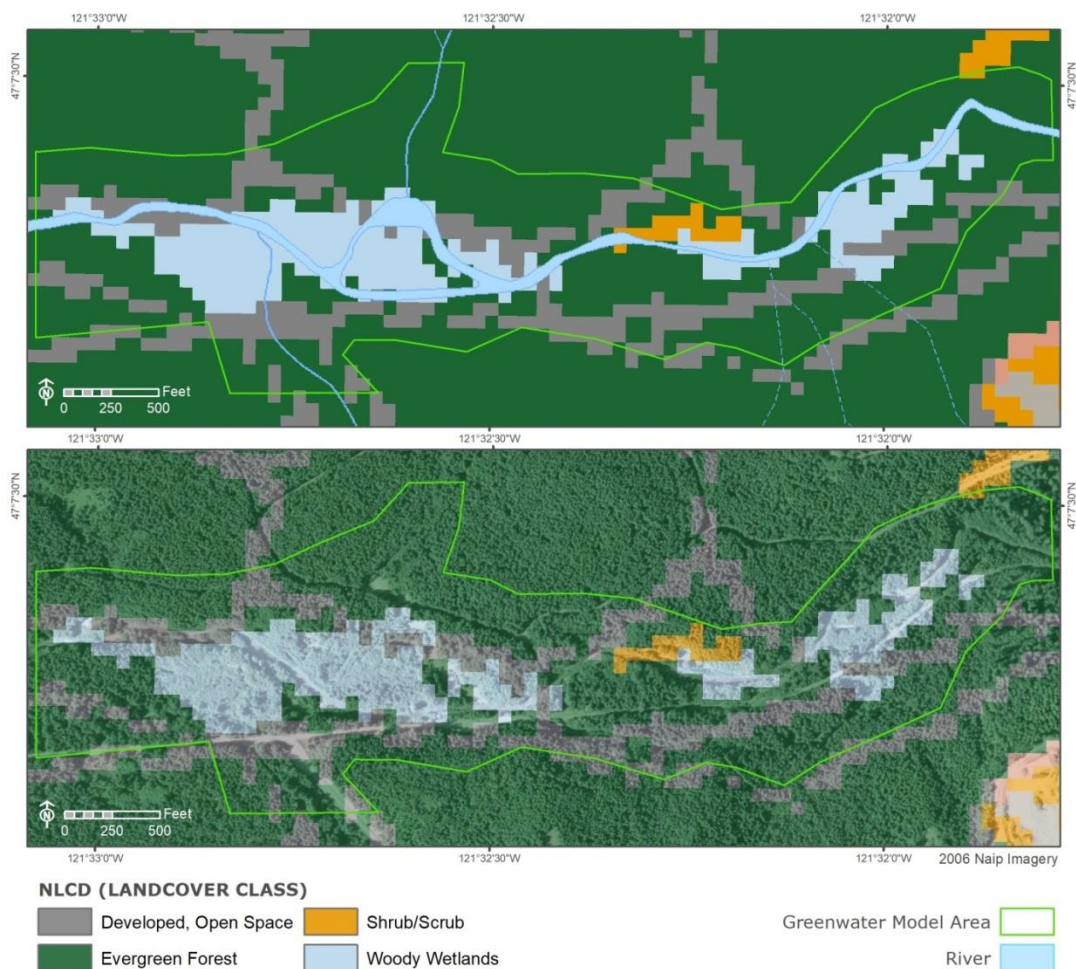


Figure 3.5. National Land Cover Dataset within the Greenwater project area

Manning's roughness values across the project area were delineated for this research using a combination of HECI (2010) roughness values, aerial imagery, vegetation height models, DTM, and DTM slope. See Figure 3.6 for a sample of these inputs. Manning's n tables from Chow (1959) were referenced to validate final roughness value determinations, while the above inputs were primarily used to digitize precise areas of land cover. Manning's n roughness values used in the HECI (2010) model—determined through field investigations, expert experience and knowledge of roughness values used in other modeling projects in the area—were utilized as a starting point for roughness determinations. HECI roughness was provided as a static map that was georeferenced into ArcGIS to be used as a starting template for delineation of the various land cover areas. Areas were drawn within the ArcGIS environment. By toggling between the above mentioned layers within ArcGIS, the new land cover areas were drawn and appropriate Manning's n roughness values were assigned. The following describes the use of the various layers utilized to assign roughness areas and values.

Vegetation heights are useful for parameterizing surface roughness for use in hydraulic models (Mason et al., 2003). Vegetation height maps were created by subtracting the bare-earth DTM from the highest hit DSM in ArcGIS. This provides a top surface height of vegetation and other features relative to ground level. Land cover type and density were estimated from the vegetation height map in conjunction with aerial imagery. The DTM and the visualization of DTM slope are useful to identify channels and their banks when delineating these areas of land cover. Only features within the area

to be modeled were delineated, and features such as roads outside of the Greenwater River floodplain and its tributary inflows were not identified.

Land cover designations for the 2017 model were created in a similar fashion to those determined for the 2007. Manning's n values associated with log jams was guided by Dudley, Fischenich, & Abt (1998) which stated that Manning's n values increase 39% when woody debris is present. Channel roughness of $n=0.55$ was multiplied by this factor to yield a roughness of $n=0.076$ for log jams.

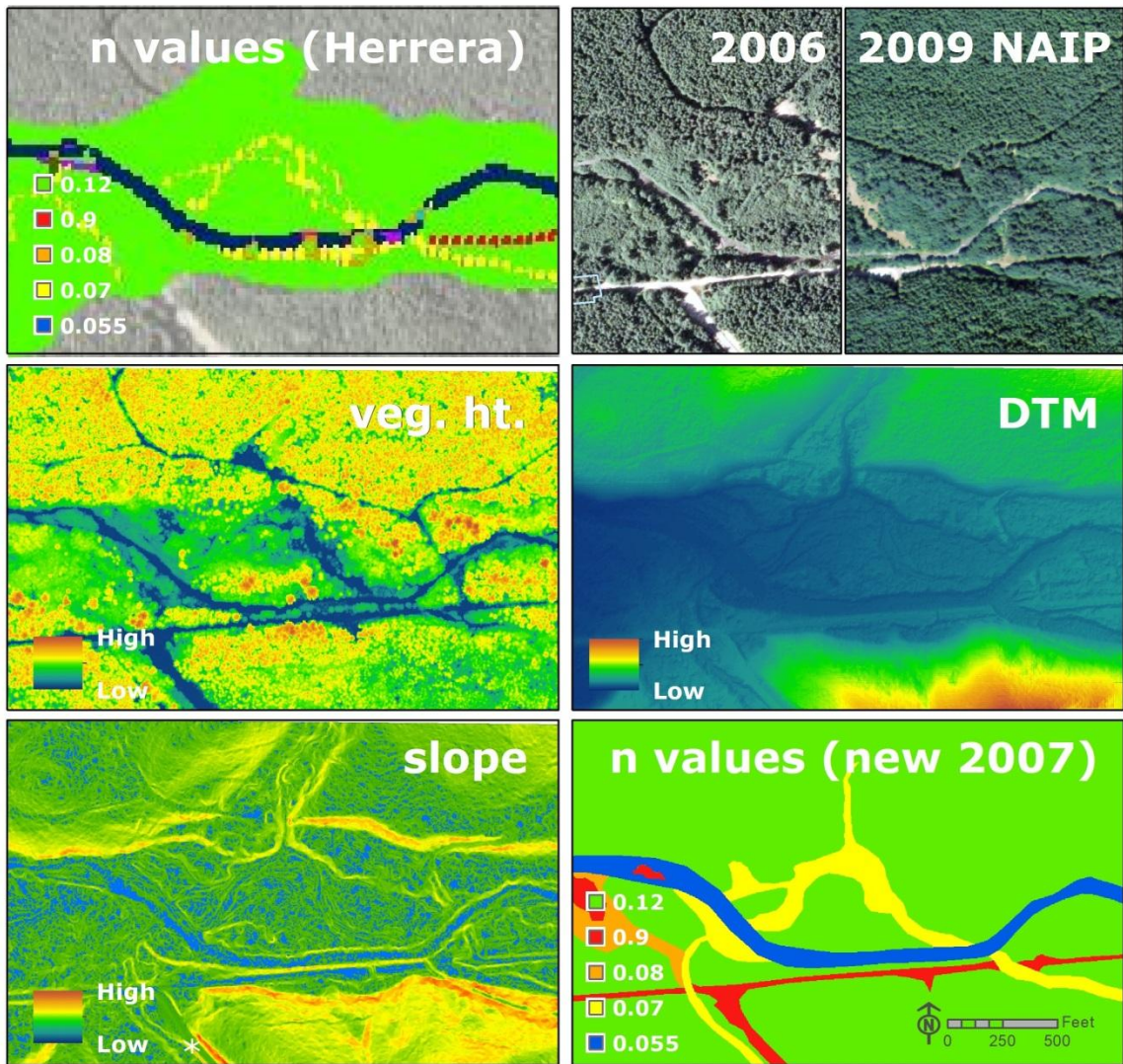


Figure 3.6. Sample of data used to delineate Manning's n roughness values

Once all of the necessary data were collected and prepared, hydraulic models of the project reach were developed. A detailed description of the parameters of the HEC-RAS hydraulic model can be found in the next section.

3.4 Modeling

Hydraulic modeling for this research was done using HEC-RAS 5.0.3. Modeling was performed using the 2007 and 2017 lidar at various flood stages and at different resolutions of the 2017 data. This section discusses the modeling process and specifications.

Preprocessing of model inputs was done in ArcGIS. To prepare the bare-earth lidar DTMs for input into the hydraulic model, the area of interest, including the river, major tributary inflows and the surrounding floodplain, were delineated. This determination was assisted by following contours well above the floodplain to specify the project area. The lidar DTM was then clipped to the project area and output in GeoTIFF format for direct input into HEC-RAS.

When starting a new HEC-RAS project, a projection file must be designated before any terrain data can be imported. The Greenwater project area is located within two US State Plane projection zones, although the river and the majority of the floodplain are located in the northern zone. The projection was set to the NAD83 Washington State Plane North FIPS 4601 projected coordinate system. This is also the native projection of the pre-project lidar data (Watershed Sciences, 2007). The lidar DTM could then be imported into HEC-RAS as a new terrain layer.

HEC-RAS allows for the combination of 1D cross-section data, portraying the topography under the water surface, with a 2D terrain. No cross-section data were

available from 2007, so the hydraulic model was run as a 2D model only and not a combined 1D/2D model. Without blue-green bathymetry lidar to accurately describe the subsurface terrain, the lidar DTM depicts increased smoothing and a generalized slope in areas covered by water. This can be mitigated within the modeling environment by using informed Manning's roughness values (Crowder & Diplas, 2000). The land classification data set with established Manning's n values described in the above section was hence imported into the model.

The 2017 data were also run as a 2D model to allow for comparisons to be made. It should be noted that there was less effect on the 2017 data by the lack of bathymetry, as the flows were lower during the 2017 lidar flight, exposing more of the channel topography. Captured at a higher resolution, the 2017 data also reveal more fine-scale topographic features within the channel that affect water movement.

Within HEC-RAS geometry editor, the 2D-flow area is delineated. High ground contour lines well outside the possible flow area were again used to select an area that included the entire floodplain. The 2D-flow area describes the boundaries of the model and contains the computational mesh. HEC-RAS uses an implicit finite-volume solution scheme to calculate flow within the 2D-flow area. The algorithm provides improved stability and robustness over more traditional finite difference and finite element techniques, and was developed to work with both a structured or unstructured computation mesh (Brunner, 2016). This allows computations to be made across a standard gridded mesh with 4-sided cells or one that contains a combination of polygons with a mixture of 3–8 sides. Various polygonal shapes are created along the border of the 2D-flow area and along breaklines within the flow area. See Figure 3.7.

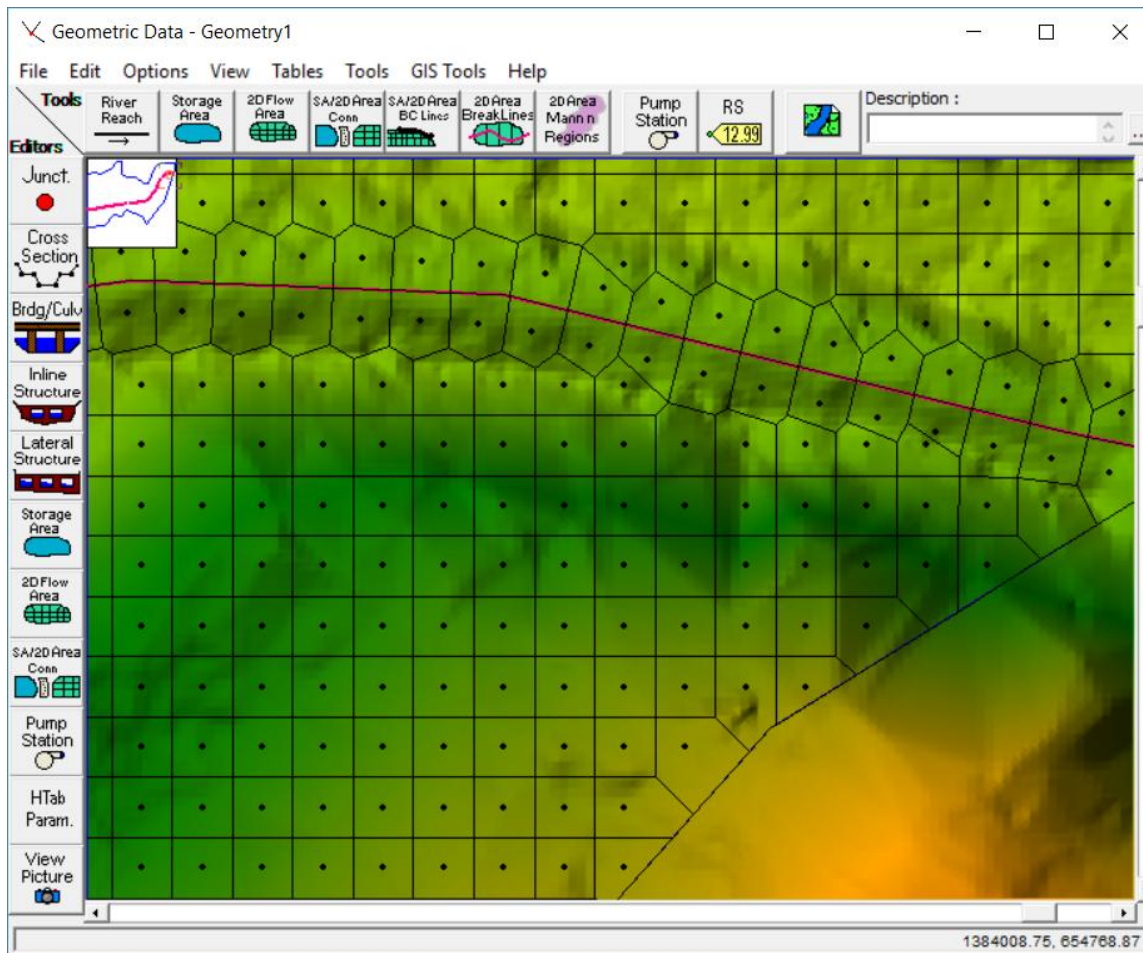


Figure 3.7. Depiction of combined structured and unstructured computational mesh. Breakline along FR 70 road surface is in red.

Breaklines are added to insure that computational cell faces align properly to capture high-ground features. It is recommended to add break lines along levees, roads, and high-ground features (Brunner, 2016). Breaklines were added to the 2007 flow area along the top surface of the road prism that was later removed during restoration.

The computational mesh was generated on regular intervals with all breaklines. Cells of the computational mesh in HEC-RAS do not have a flat-bottom, single elevation, as do some other hydraulic models. Instead HEC-RAS 2D modeling uses a high-resolution, subgrid model where each cell face is similar to a detailed cross-section, and

cells and cell faces are preprocessed with detailed hydraulic property tables (elevation versus area, wetted perimeter, and roughness) based on the underlying terrain (Brunner, 2016). See Figure 3.8. This allows for cells to be partially wetted, providing detailed subgrid level precision to model outputs through the retention of terrain detail while implementing larger computational cells, resulting in faster model run times. A computation point spacing of 10 feet was used for this research. After the computational mesh was defined, flow inputs and outputs were established along the boundary of the 2D flow area.

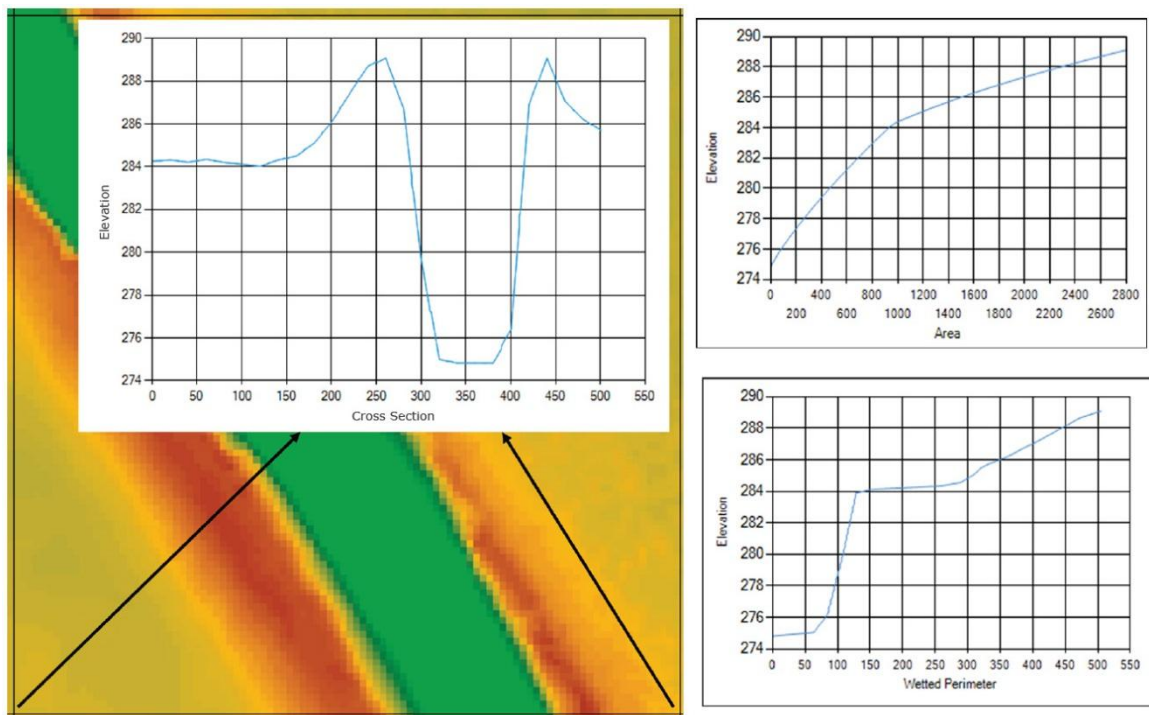


Figure 3.8. Example of cell and cell face detailed hydraulic tables (Brunner, 2016)

Within the project area, the Greenwater River flows primarily from east to west, with one tributary coming in from the north and another from the south. Boundary conditions are identified to bring flow into and out of the modeled area. The model

inflows are identified across the channel at the upstream end of the Greenwater River and the two tributaries, while the outflow is delineated across the entire floodplain at the downstream end of the project area. Peak flood discharge values run through the model inflows were adjusted from the Greenwater USGS gage number 12097500, as seen in Table 3.1.

The model was run on the 2007, 2017, and downsampled 2017 DTM for the mean annual minimum, mean annual, 1-year, 1.6-year (bankfull), 2-year, 5-year, 10-year, 25-year, 50-year, and 100-year flow events. The default diffusion wave equations were used, allowing the model to run faster and have increased stability (Brunner, 2016).

3.5 Results Analysis

Model results were exported from HEC-RAS and imported into ArcGIS for analysis. Results between pre- and post-project conditions were compared at specific flow events to determine the overall effectiveness as well as how the project held up to predictions made in the HECI (2010) proposed conditions assessment. The inundation area for each flow event was calculated in order to determine the gain in wetted area. Visual inspection of specific events provides insight into morphological changes that have caused an increase in floodplain and side channel activation. Mean flow velocities as well as local patterns in flow velocity were investigated for the 10-year and 100-year events. Finally, a comparison between the native resolution and downsampled 2017 terrain was made to explore the effects of lower resolution DTM on hydraulic model outputs.

4.0 RESULTS

4.1 Introduction

The results of this research first answer the question of the effectiveness of the Greenwater River Floodplain Restoration Project to achieve floodplain connectivity and velocity reduction goals. This project removed a section of Forest Road 70, previously separating the river from part of its floodplain, and added several ELJs within the river. All ELJs are still intact and functioning at the time of this study. Hydraulic modeling performed for this research analyzes the effect of project changes to the landscape on water flow throughout the restoration area. A comparison is made between the pre-project (2007) and the post-project (2017) inundation areas and velocities for a range of flow events from the mean annual minimum to the 100-year flood.

Differences in inundation area and mean velocity are also compared between the native 1-foot resolution of the post-project DTM and the same dataset downsampled to 3-foot grid cells, the pre-project DTM resolution. This was done to answer whether there is any difference in modeled floodplain delineation at the reach scale with this level of resolution difference. It gives some insight into benefits of the higher resolution digital elevation model produced from a drone flight as compared to the lower resolution elevation model that would be output from lidar flown by manned aircraft.

Maps of the hydraulic model results are broken up into 4 zones labeled A, B, C, and D, following flow direction from east to west. Zones were established to aid in the discussion of specific features and changes in flow patterns. Zone A includes the upper side channel/floodplain connection and 3 ELJs. See Figure 4.1. Zone B includes the side channel, known as the “wall-based side channel” by project managers, and 2 ELJs. Zone

C includes the historic channel connection, the Slide Creek confluence with the Greenwater River, and the majority of ELJs. Zone D includes the 28 Mile Creek confluence, the lower floodplain, and the final ELJ.

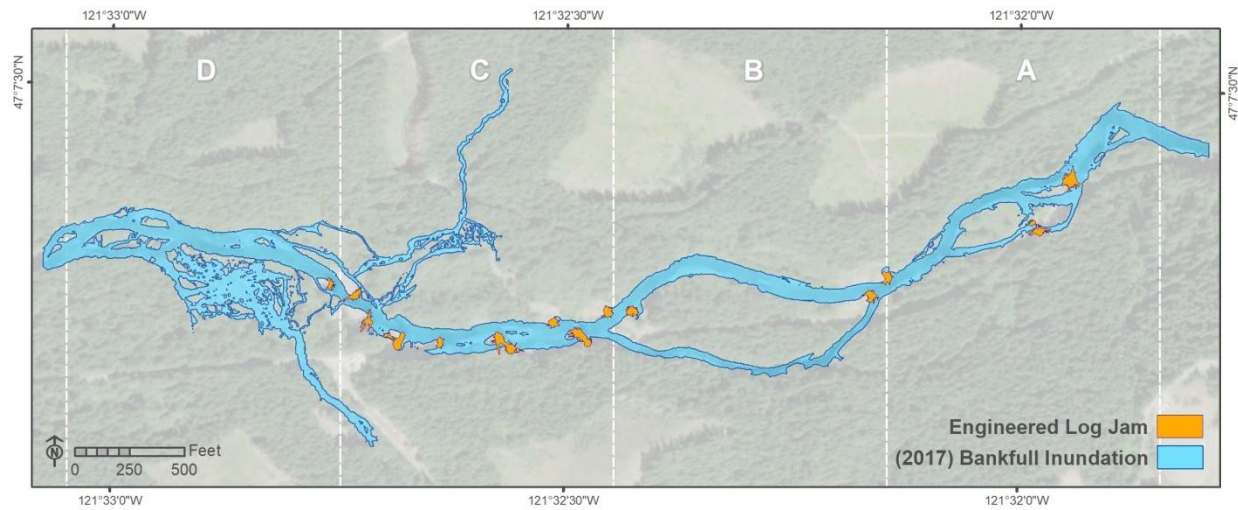


Figure 4.1. Engineered log jam locations shown on the post-project bankfull inundation

Results are organized as follows. First, inundation area is compared across all flow events on the pre- and post-project landscape. Inundation area of individual events comparing pre- and post-project conditions for the mean annual minimum, 1.6, 5, 10, 25, 50, and 100-year flow events are examined to identify changes to flow patterns and floodplain activation. Velocities are compared for the 100- and 10-year flow pre- and post-project across the entire floodplain as well as specifically within the mean annual minimum inundation area, where the scour effect on salmon redds would be greatest. Finally, digital elevation model resolution effects on modeled floodplain delineation and velocities are explored to identify effects of a higher resolution terrain on modeled results.

4.2 Inundation Area

The inundation area is the area of land covered by water. Inundation area was modeled for specific flow events including the mean annual minimum flow, mean annual flow, 1, 1.6 (bankfull), 2, 5, 10, 25, 50, and 100-year floods. Inundation areas were calculated within the Greenwater River floodplain only and do not include the 2 tributaries' inflow areas.

A comparison of inundation area for all flow events is illustrated in Figure 4.2. Wetted area within the project boundary ranges from 8.6 acres for the Mean Annual Minimum flow, modeled on the 2007 landscape, to 47.7 acres for the 100-year flood event, modeled on the 2017 landscape. All flow events show an increase in inundation area on the 2017 post-project landscape. The area increase from 2007 to 2017 showed a relatively narrow range of change across all events, from 1.5 acres for the 25-year flood to 3.6 acres for the 100-year flood. The percent area increased ranged from 4.5% for the 25-year flood to 31.2% for the mean annual minimum flood. Events below the 1.6-year bankfull flow showed area changes averaging 2.6 acres, but revealed the greatest percent increase in area ranging from 21.7% to 31.2% and averaging 26.7%. Events at bankfull flow and above showed similar area increases, averaging 2.4 acres, but revealed smaller percent area increases ranging from 4.5% to 12.4% and averaging 9.0%.

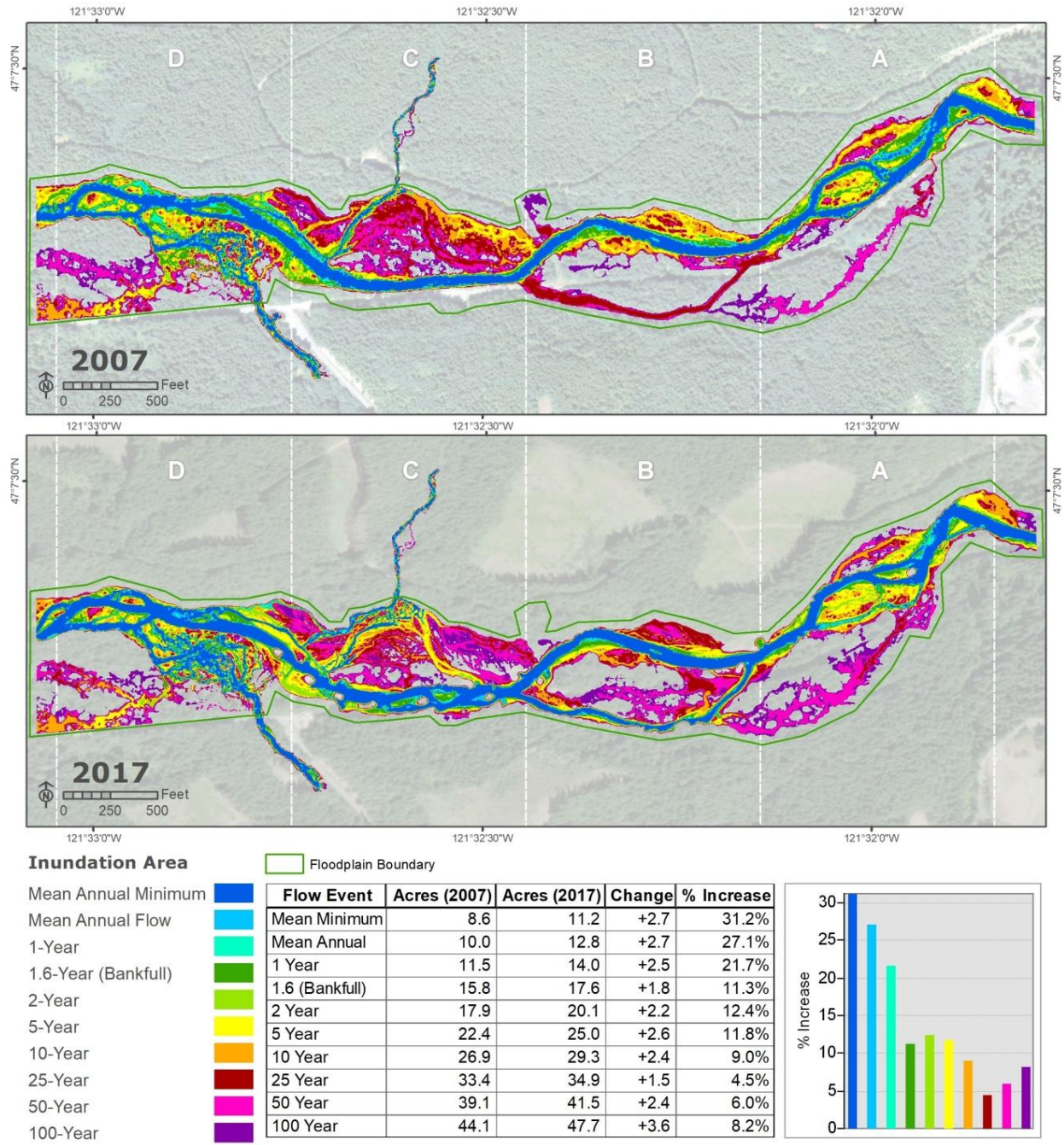


Figure 4.2. Inundation areas for all flood events

4.2.1 Inundation Area - Mean Annual Minimum

The mean annual minimum flow is representative of flow rates during spawning months of Spring Chinook and Coho Salmon in the Greenwater River (Ecology, 1998; Marks et al., 2016). The inundation area for the mean annual minimum flow, shown in Figure 4.3, increased 2.7 acres, from 8.6 to 11.2 acres. This represents a 31.2% increase in wetted area. Zone A shows some local changes in flow patterns likely due to log jam placements. A comparison between the mean annual minimum inundation areas show the approximately 1,500-foot side channel in zone B is now fully connected during low flow conditions post-project. During pre-project conditions this side channel did not connect until somewhere between the 10- and 25-year events. This is one of the most notable and significant changes in post-project conditions for the mean annual minimum flow. Zones C and D reveal a wider, more braided channel post-project, presenting more potential spawning area for fish and increased potential for wood and sediment recruitment.

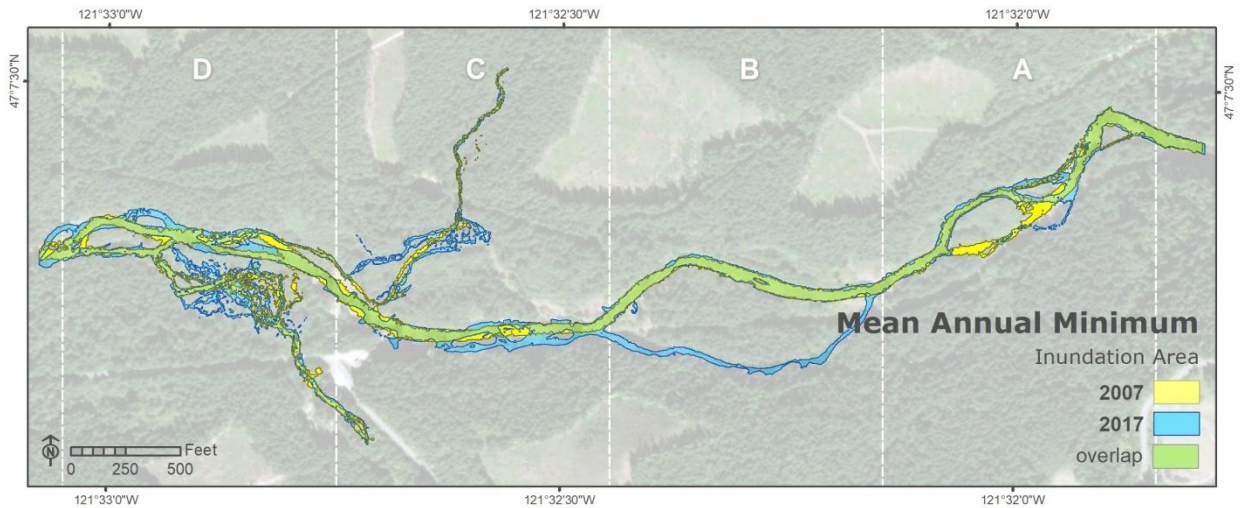


Figure 4.3. Mean annual minimum inundation areas pre- and post-project

4.2.2 Inundation Area – Bankfull

Bankfull flow represents the stage at which the water level tops the channel before it spills out into the floodplain. The inundation area for the 1.6-year bankfull flow, shown in Figure 4.4, increased 1.8 acres, from 15.8 to 17.6 acres. This represents an 11.3% increase in wetted area. Zone A shows a connection of the smaller side channels in the upper project area. In zone B, the channel has become slightly wider as it fills in. Zones C and D see more braiding across the floodplain of the tributary inflows of Slide and 28 Mile Creeks along, with a filling in of the main Greenwater channel.

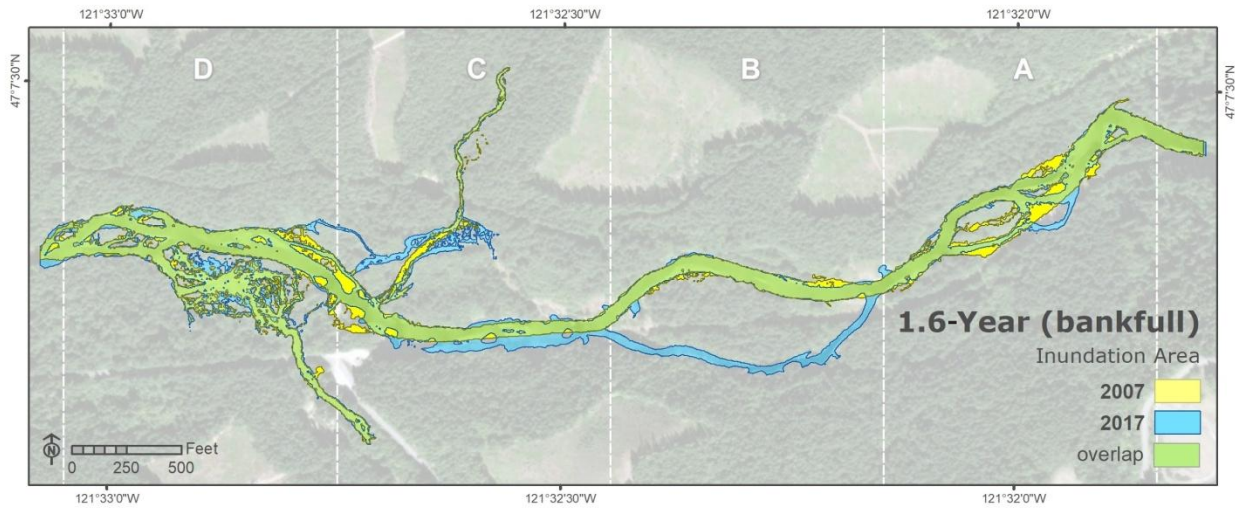


Figure 4.4. 1.6-year bankfull inundation areas pre- and post-project

4.2.3 Inundation Area – 5-Year

The inundation area for the 5-year flow, shown in Figure 4.5, increased 2.6 acres, from 22.4 to 25.0 acres. This represents an 11.8% increase in wetted area. Zone A shows a filling in of the upper channel. Flows in zone B have started to spill slightly into the floodplain. The connection with the historic channel, that joins the Greenwater River to Slide Creek higher up and more to the north, is seen in zone C. This connection is more consistent with the original channel on the new post-project landscape. The floodplain in zone D has begun to fill in at the 5-year flood.

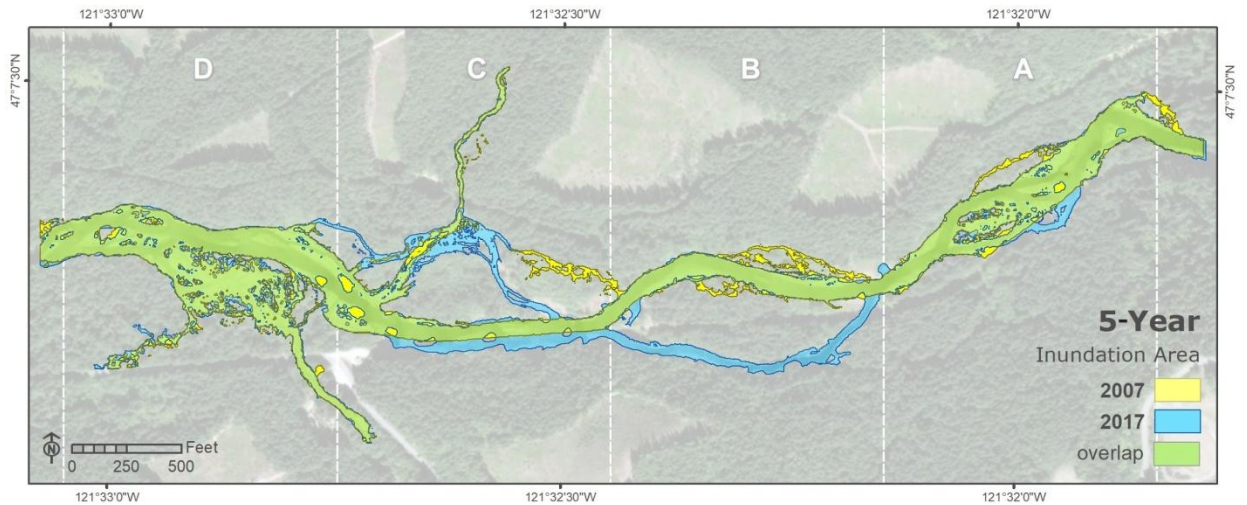


Figure 4.5. 5-year inundation areas pre- and post-project

4.2.4 Inundation Area – 10-Year

Occurrences of the 10-year flood have been observed to have increased in the last 10 years (USGS, 2018). The inundation area for the 10-year flow, shown in Figure 4.6, increased 2.4 acres, from 26.9 to 29.3 acres. This represents a 9.0% increase in wetted area. All zones are observed to be spreading out into the floodplain. The most notable difference between pre- and post-project conditions, not already noted, is a more defined connection within the historic channel in zone C.

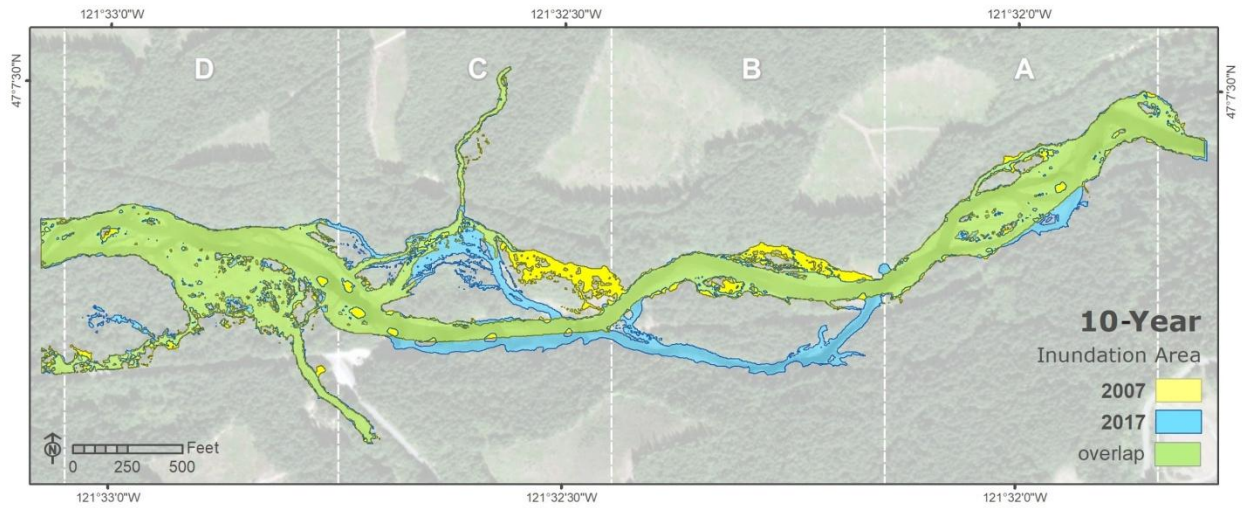


Figure 4.6. 10-year inundation areas pre- and post-project

4.2.5 Inundation Area – 25-Year

The inundation area for the 25-year flow, shown in Figure 4.7, increased 1.5 acres, from 33.4 to 34.9 acres. This represents a 4.5% increase in wetted area. Zone A shows the beginning of the connection of an upper side channel on the post-project terrain. In Zone B, the pre-project, wall-based side channel would now be activated through small openings in Forest Road 70 made in a previous, smaller scale restoration effort that removed sections of the road where culverts had previously been. Before the Greenwater River Floodplain Restoration Project, this was the only method for water to reach that section of floodplain. Pre-project flow patterns are now spilling into the historic channel in zone C. Post-project conditions are resulting in more flow spilling out of the channel onto the floodplain across zones B, C, and D.

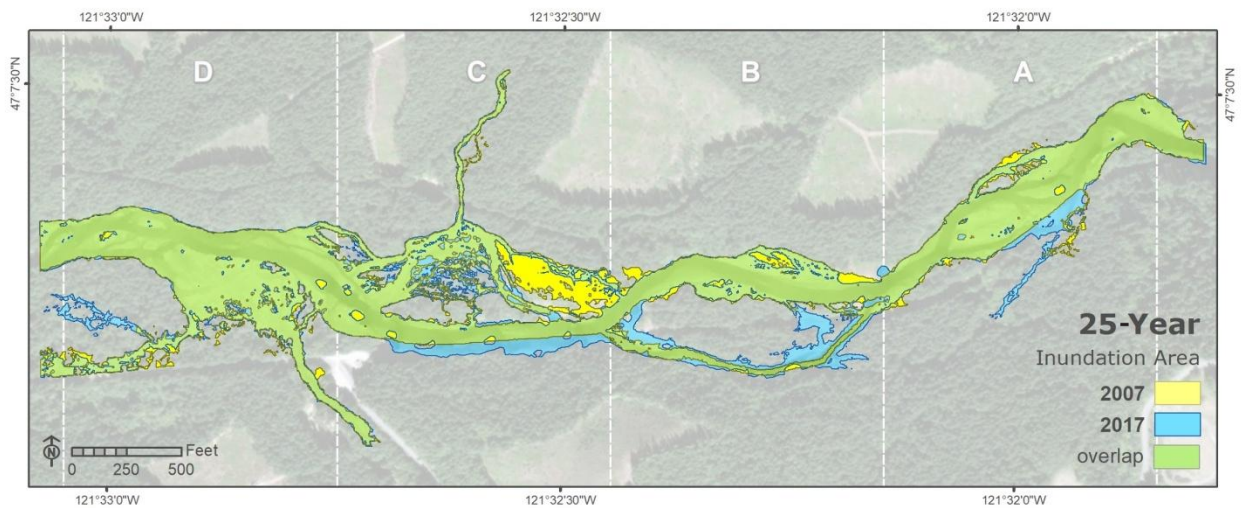


Figure 4.7. 25-year inundation areas pre- and post-project

4.2.6 Inundation Area – 50-Year

The inundation area for the 50-year flow, shown in Figure 4.8, increased 2.4 acres from 39.1 to 41.5 acres. This represents a 2.4% increase in wetted area. Zone A shows the connection of the upper side channel. More activation around the side channels of the southern floodplain is seen in both zones A and B, post-project. Zone C and D both have similar floodplain activation at the 50-year flood pre- and post-project.

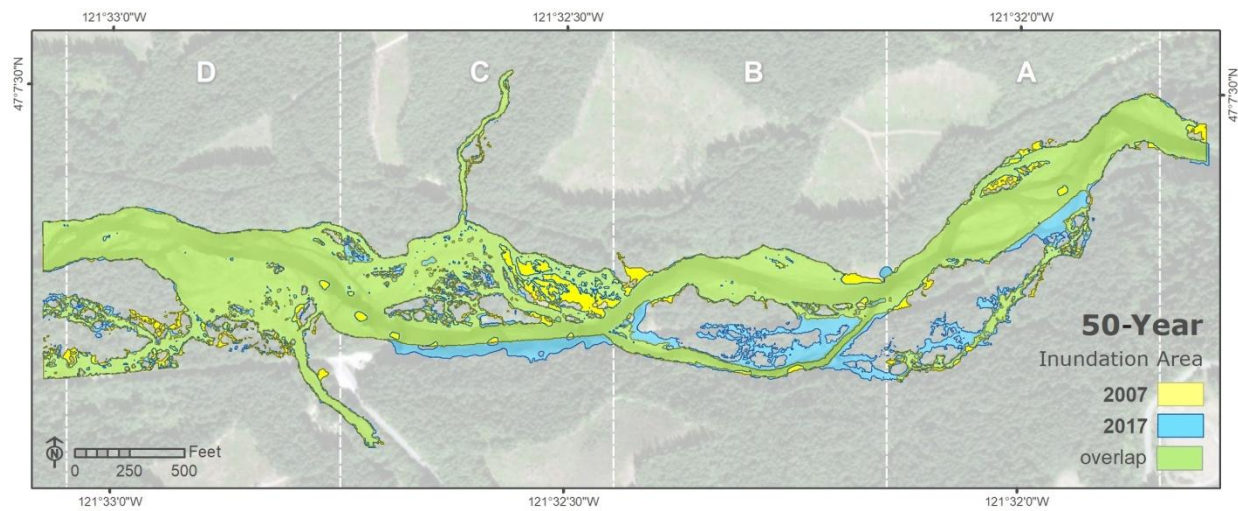


Figure 4.8. 50-year inundation areas pre- and post-project

4.2.7 Inundation Area – 100-Year

The inundation area for the 100-year flow, shown in Figure 4.9, increased 3.6 acres from 44.1 to 47.7 acres. This represents an 8.2% increase in wetted area. Zone A and B again display more of the southern floodplain activation post-project. Zone C and D show similar floodplain activation at the 100-year flood pre- and post-project.

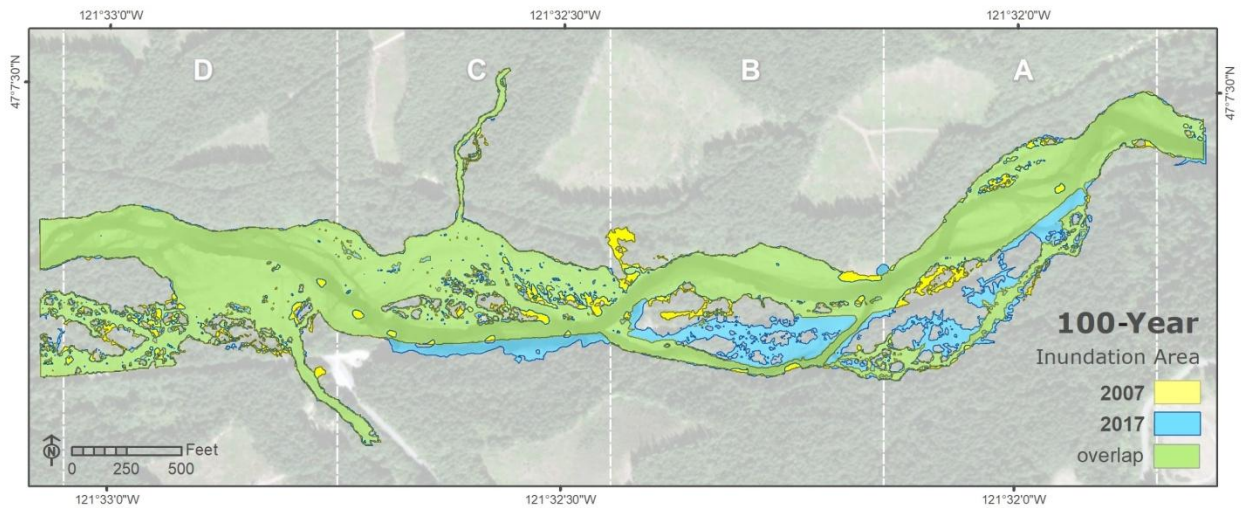


Figure 4.9. 100-year inundation areas pre- and post-project

4.3 Flow Velocity

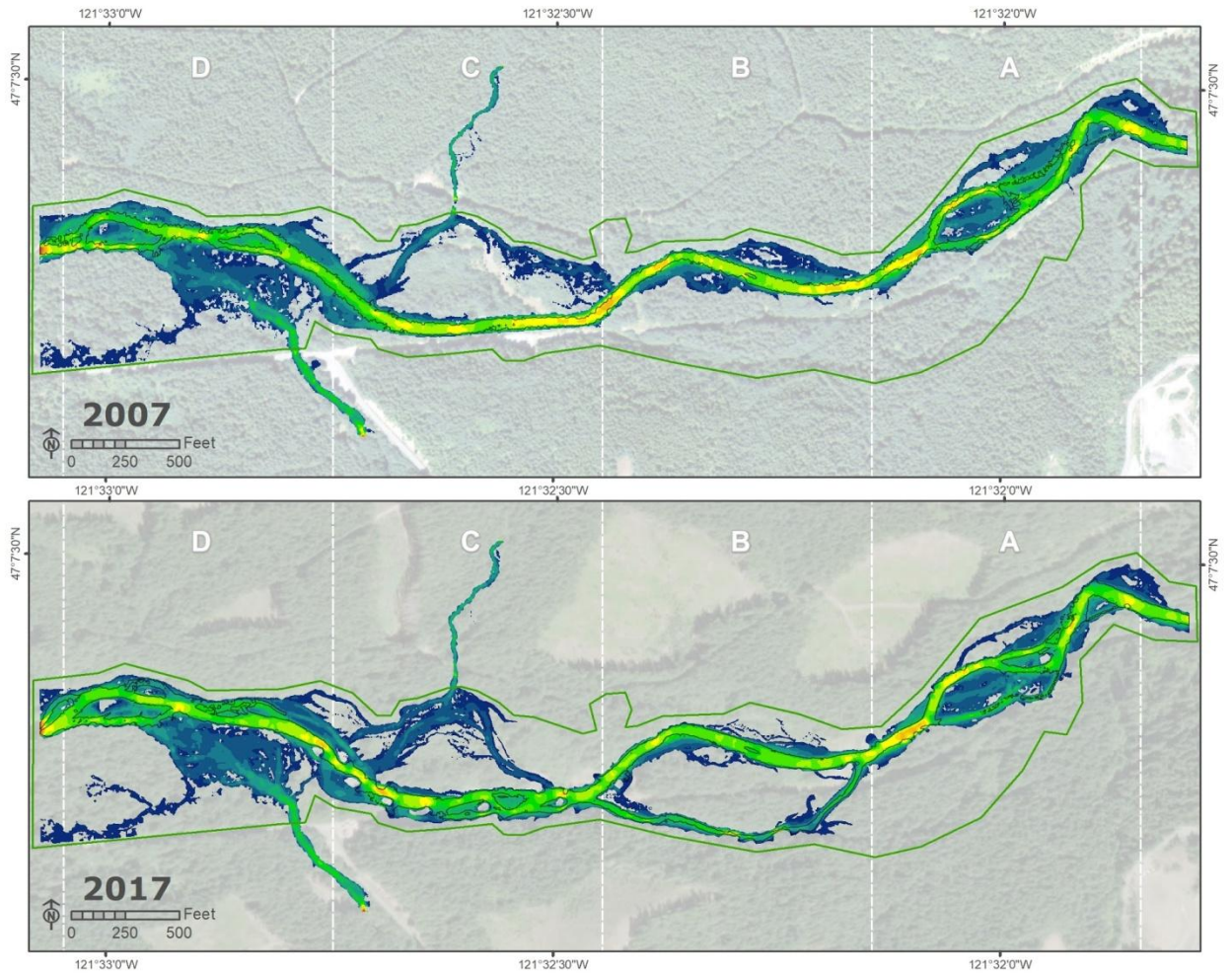
Flow velocities were analyzed for the 10 and 100-year events. The 10-year event represents a relatively frequent flooding event. The 100-year event represents extreme flooding. Flow velocities were analyzed only within the Greenwater River floodplain and do not include the 2 tributaries' inflow areas. Velocities were compared both across the entire wetted area as well as within the theoretical spawning channel, represented by the mean annual minimum inundation area, in an effort to explore the possible effect of more frequent flood events on salmon redds.

4.3.1 Flow Velocities – 10-Year

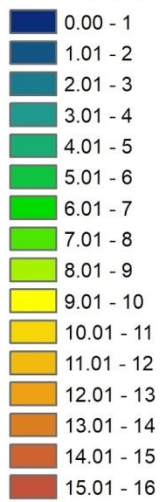
The 10-year flow velocities, shown in Figure 4.10, modeled on the post-project landscape, show a decrease in velocities by 1.57% across the entire channel and floodplain, while a 9.16% decrease is modeled within the spawning channel. See Table 4.1. In a Welch's two sample t-test, the difference between the means is significantly different, $p < 0.001$, for both areas.

Table 4.1. 10-year velocities pre- to post-project

10-Year Flood							
Floodplain				Spawning Channel			
2007 Mean Velocity (ft/sec)	2017 Mean Velocity (ft/sec)	Velocity Change	% Decrease	2007 Mean Velocity (ft/sec)	2017 Mean Velocity (ft/sec)	Velocity Change	% Decrease
3.82	3.76	-0.06	-1.57%	7.53	6.84	-0.69	-9.16%
$\sigma = 2.91$	$\sigma = 2.74$			$\sigma = 1.64$	$\sigma = 1.78$		



10-Year Velocity (ft/sec)



Spawning Area *
 Floodplain Boundary

*Greenwater Mean Minimum Annual Flow Wetted Area

% Decrease in Mean Velocity (2007-2017)	
Floodplain	Spawning Channel
-1.57%	-9.16%

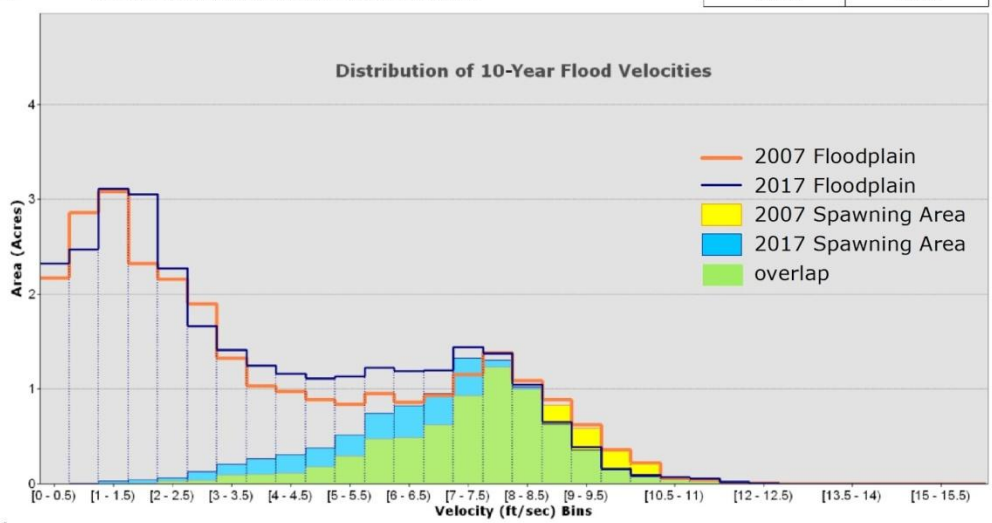


Figure 4.10. 10-year velocities pre- and post-project

4.3.2 Flow Velocities – 100-Year

The 100-year flow velocities, shown in Figure 4.11, modeled on the post-project landscape, show a decrease in velocities by 3.83% across the entire channel and floodplain, while an 8.46% decrease is modeled within the spawning channel. See Table 4.2. In a Welch’s two sample t-test, the difference between the means is significantly different, $p < 0.001$, for both areas. The visualization of flow velocities shows more continuous high velocity flows in the pre-project channel, while in post-project conditions velocities are seen to occur in sequence broken up by lower velocity regions which would give rearing fish some refuge from higher velocities, and theoretically help protect salmon redds in the area from scour.

Table 4.2. 100-year velocities pre- to post-project

100-Year Flood							
Floodplain				Spawning Channel			
2007 Mean Velocity (ft/sec)	2017 Mean Velocity (ft/sec)	Velocity Change	% Decrease	2007 Mean Velocity (ft/sec)	2017 Mean Velocity (ft/sec)	Velocity Change	% Decrease
4.18	4.02	-0.16	-3.83%	9.93	9.09	-0.84	-8.46%
$\sigma = 3.36$	$\sigma = 3.33$			$\sigma = 1.96$	$\sigma = 2.23$		

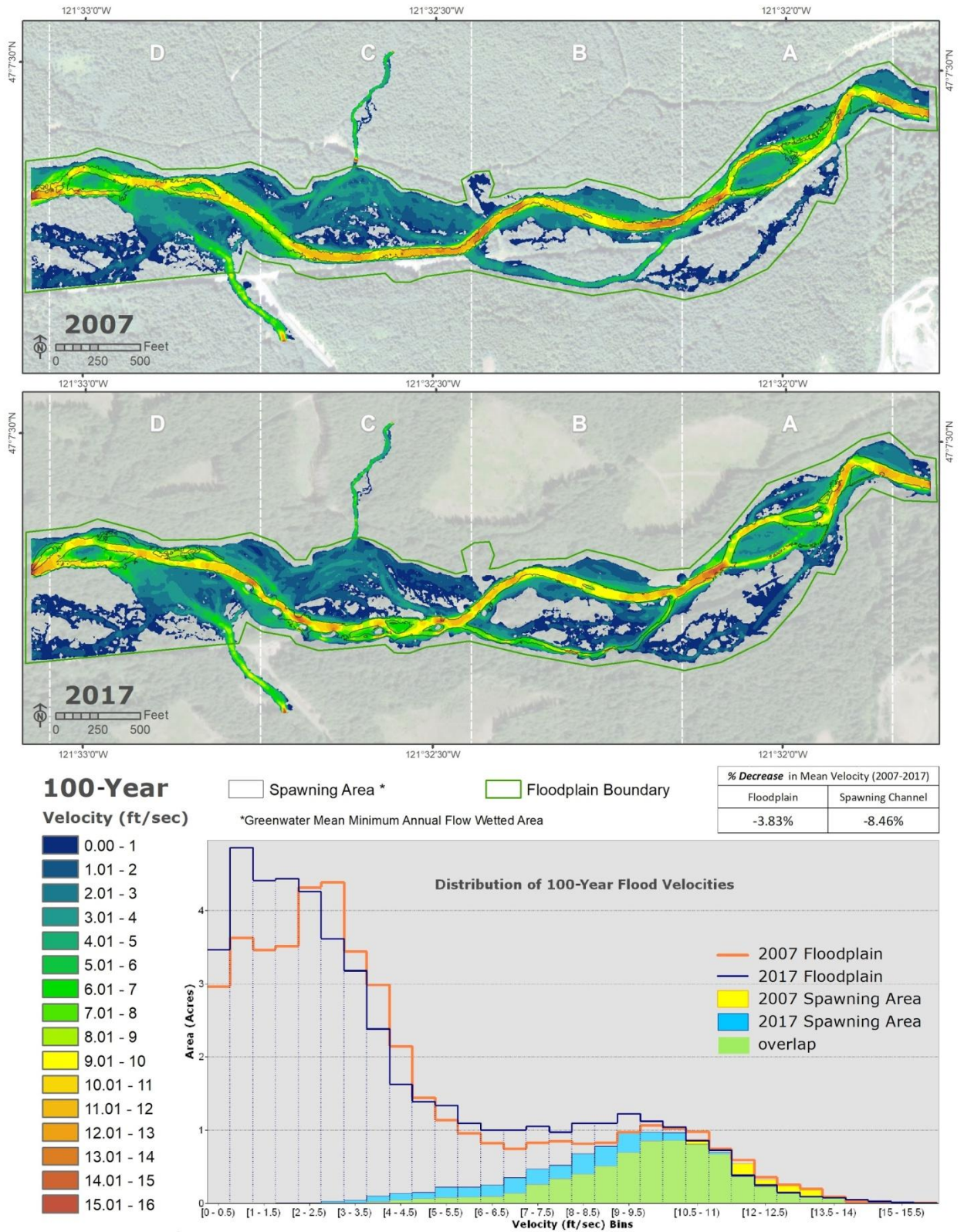


Figure 4.11. 100-year velocities pre- and post-project

4.4 DTM Resolution Effect on Hydraulic Modeling

Digital terrain data for the 2017 post-project conditions were downsampled from a 1-foot to a 3-foot raster grid, and hydraulic modeling was then performed on the downsampled 3-foot gridded terrain, to determine any difference in modeled outputs at this magnitude of difference. Very small variations were observed in the spatial patterns of the modeled inundation areas for all events. Similar to the other event results, the 100-year flood inundation area, seen in Figure 4.12, displays almost the entire inundation area modeled on the 1-foot and 3-foot terrain as overlapping, with only small areas of difference peeking out in the off-channel floodplain areas, resulting in a 1.34% change in area. A comparison between inundation areas for all events is presented in Table 4.3.

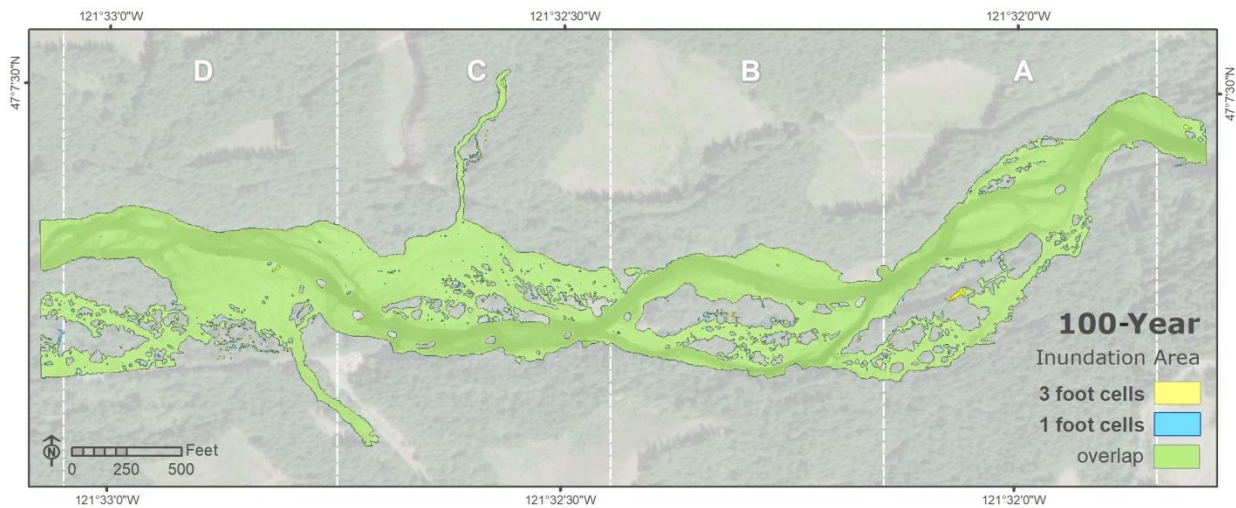


Figure 4.12. 100-year inundation areas on post-project 1-foot and 3-foot gridded terrain

Table 4.3. Inundation areas on post-project 1-foot and 3-foot gridded terrain

Flow Event	Inundation Area			
	Acres (1-foot)	Acres (3-foot)	Change	% Decrease
Mean Annual Minimum	11.2	10.5	-0.69	6.13%
Mean Annual	12.8	12.0	-0.79	6.13%
1-Year	14	13.2	-0.78	5.56%
1.6-Year (Bankfull)	17.6	17.0	-0.57	3.22%
2-Year	20.1	19.4	-0.69	3.42%
5-Year	25	24.3	-0.66	2.63%
10-Year	29.3	28.6	-0.66	2.26%
25-Year	34.9	34.1	-0.76	2.17%
50-Year	41.5	40.6	-0.91	2.18%
100-Year	47.7	47.1	-0.61	1.28%

All flow events show a decrease in inundation area on the downsampled 3-foot landscape. The area decrease was similar across all events, ranging from 0.57 acres for the 1.6-year flood to 0.91 acres for the 50-year flood, with a standard deviation of 0.09 acres. The percent area decrease ranged from 1.28% for the 100-year flood to 6.13% for the mean annual minimum and the mean annual flows, consistently decreasing as discharge and inundation area increases. Even though the percent decrease was larger for the lower flow events the spatial patterns remain very similar, as seen in the inundation areas for the mean annual minimum event, shown in Figure 4.13

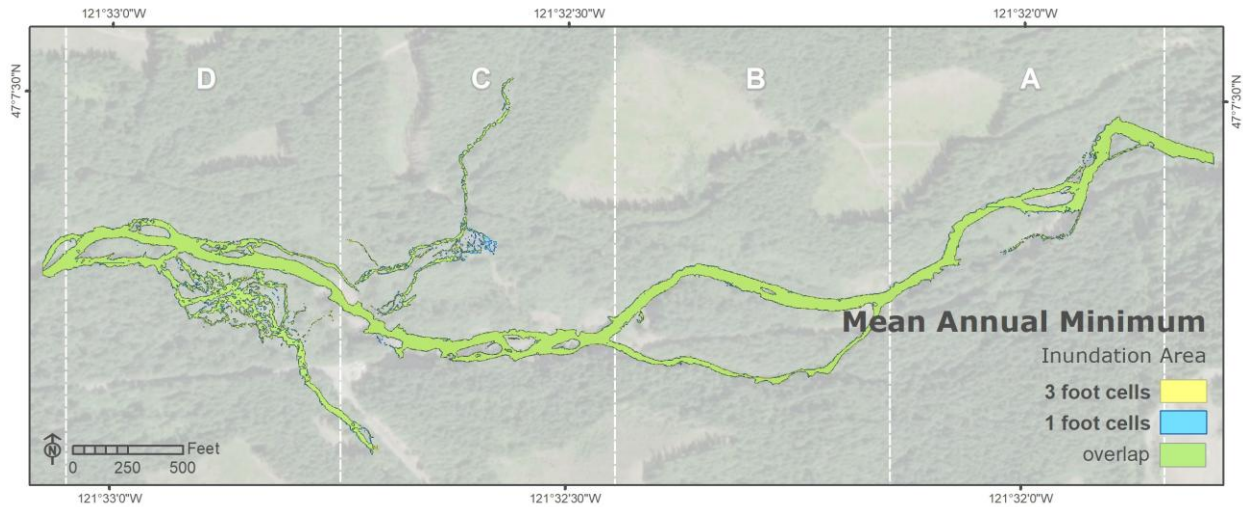


Figure 4.13. Mean annual minimum inundation areas on post-project 1-foot and 3-foot gridded terrain

A comparison between velocities modeled for the 10 and 100-year events on the 1-foot and 3-foot terrain is presented in Table 4.4. Results show no greater than a 0.5% change in mean velocities, with a slightly negative change observed over the entire floodplain, and a slightly positive change seen within the spawning channel.

Table 4.4. Mean velocities on post-project 1-foot and 3-foot gridded terrain

100-Year Flood							
Floodplain				Spawning Channel			
1 foot Mean Velocity (ft/sec)	3 foot Mean Velocity (ft/sec)	Velocity Change	% Change	1 foot Mean Velocity (ft/sec)	3 foot Mean Velocity (ft/sec)	Velocity Change	% Change
4.02	4.00	-0.02	-0.50%	9.09	9.11	0.02	0.22%
$\sigma = 3.33$	$\sigma = 3.32$			$\sigma = 2.23$	$\sigma = 2.19$		
10-Year Flood							
Floodplain				Spawning Channel			
1 foot Mean Velocity (ft/sec)	3 foot Mean Velocity (ft/sec)	Velocity Change	% Change	1 foot Mean Velocity (ft/sec)	3 foot Mean Velocity (ft/sec)	Velocity Change	% Change
3.76	3.75	-0.01	-0.27%	6.84	6.86	0.02	0.29%
$\sigma = 2.74$	$\sigma = 2.75$			$\sigma = 1.78$	$\sigma = 1.76$		

5.0 DISCUSSION

“all models are wrong, but some are useful”

-George E. P. Box, 1976

5.1 Introduction

Results of the hydraulic modeling show that the Greenwater River Floodplain Restoration Project had a positive effect on floodplain reconnection and reduction of velocities within the channel across all flow events modeled. Combined with other floodplain enhancement projects in the area, the Greenwater River project should add resiliency to this watershed, increasing available ecologically functioning habitat for salmon while reducing flooding risk for downstream communities. As climate changes lead to shifting flow patterns, the need for an understanding of and continued effort towards floodplain restoration becomes ever more important.

Results from the analysis of terrain resolution effect on the hydraulic model, at the reach scale, show very little change in inundation and velocity outputs at the studied resolution difference. This provides evidence that UAV lidar should not be selected for project monitoring based on the hope for more accurate hydraulic model outputs alone. There are, however, other advantages to this type of acquisition, such as cost savings for smaller project areas, and the resulting higher resolution output has potential for other analysis, especially if blue-green bathymetric lidar can be acquired.

This chapter first discusses the results of the modeled inundation and velocity comparisons. The ecological importance of floodplain restoration as it relates to trending changes in flood occurrences in the Greenwater Basin is then analyzed. Next, the

comparison between modeled results on different terrain resolutions is discussed, a lidar cost comparison is presented, and finally recommendations for future research are made.

5.2 Pre- to Post-Project Comparisons

Results from this study were analyzed on their own as well as being compared to those from the pre-project HECI, 2010 assessment. Modeled results from this study were analyzed for numerical area and velocity differences pre- to post-project along with spatial flow pattern shifts resulting from changes to the morphology of the river and floodplain. When comparing models run for this study to the 2010 HECI assessment, three significant differences should be noted. One, the proposed project area at the time of the HECI assessment extended approximately an additional 1,700 feet downstream of the current project reach and lidar acquisition. Two, the HECI model input all of the calculated flow at the bottom of the project area to the inflow at the upper end of the project, while this research modeled the contributing tributary flow inputs separately rather than adding their values to the Greenwater River inflow at the top of the project. Three, the HECI model utilized peak flood levels calculated in 1996 and reported in Abbe et al. (2007), while this research used current peak flood levels reported through the USGS, that were recalculated in 2014. See Table 3.1. Results from HECI, 2010 were primarily presented graphically in the form of maps, and only the 100-year flood inundation area values were reported on. Taking into account the differences between the models, specific values would not be directly comparable. Instead, only the normalized percent increases of the 100-year event, observed floodplain and side channel activation, and velocity observations are compared between the HECI, 2010 assessment and this study.

5.2.1 Inundation Area

The removal of Forest Road 70 combined with the addition of engineered log jams throughout the project area had a notably positive effect on overall floodplain inundation area and activation of side channel habitat. Results from this study showed an 8.2% increased area for the 100-year event, with an average gain of 14.3% across all events, and a 9% gain for events above bankfull flow. These results aligned with the reported 10% increase in floodplain inundation for the 100-year event (HECI, 2010). An inspection of spatial changes to flow also revealed similar changes on the post-project terrain. Although the 2010 HECI model of the 100-year proposed conditions did show more filling in of the floodplain in zones A and B, this is likely due to higher modeled discharge inflows at the top of the project area from both a greater 100-year peak flood value and the allocation of tributary flow to the upper project area.

The most notable change to post-project inundation in this study is the activation of the wall-based side channel occurring for all events, including the mean annual minimum flow and above, which added approximately 1,500 feet of side channel habitat in zone B. This side channel did not activate on the pre-project landscape until flows exceeded the 10-year event. As expected, higher flow events also showed much more utilization of the upper floodplain in zones A and B due to removal of FR 70. Log jams installed throughout Zone C added much variation to the channel in that area, increasing potential spawning and rearing habitat throughout the main channel in that zone. As well, inspection of inundation in zone D reveals a more complex main channel due to local anabranches likely caused by the deposition of sediment leading to aggradation.

It should be noted that inundation areas reported for this research, as well as those in the HECI, 2010 assessment, are all slightly exaggerated for the specific discharge values used. This is due to the lack of bathymetry accurately depicting the topography of the channel below the water surface. Since NIR lidar does not penetrate the water surface the lidar point cloud shows no data wherever water is covering the terrain (see Appendix A & B) and the resulting DTM simply shows a flat surface between the lowest recorded points on opposite banks. This is why it was important to capture the NIR lidar during seasons of low flow, when as much of the channel as possible is visible. Discharge values used in this research represent theoretical events, which have been noted to change periodically as more gage data are collected, so a slight exaggeration of inundation is not as vital across flows modeled on the same terrain. However, this could have a slight effect on comparisons between pre- and post-project models made for this research. The 2007 Lidar was captured during a slightly higher discharge, which could skew the 2007 inundation areas to be slightly larger due to the displacement of more area under the water surface. Taking this into account would only increase the change in inundation areas, hence revealing an even more positive value for inundation area gained.

5.2.2 Flow Velocities

Modeled mean flow velocities for this study were observed to decrease for all events on the post-project 2017 terrain. Results were presented for the 10 and 100-year events. No specific values were reported for comparison in the HECI (2010) assessment, but it was stated that “velocities in the main channel significantly decrease” on the proposed project landscape, which could lead to positive post-restoration responses such as sediment deposition. Current results show that mean velocities across the entire

floodplain showed a reduction of 1.57% and 3.83% respectively. Outside of the channel, velocities are seen to be much lower than within the channel. Because there is a larger area of inundation outside of the channel than within, the difference in mean velocities across the entire inundation area are skewed to a lower value. In order to compare the changes in the higher velocities within the channel, where reductions would likely be more pronounced due to ELJ placements and morphology changes, and there would be the most effect on incubating redds, velocities were also compared for the 10 and 100-year event in the pre- and post-project mean annual minimum inundation area. An inspection of the monthly mean gage discharges (1929–2017) during the Spring Chinook and Coho Salmon spawning months of September through November yielded an average mean discharge of 102 cfs, $\sigma = 58$. Hence, the mean annual minimum event of 92 cfs at the gage was designated as an acceptable representation of the spawning channel for this research. Mean velocities in this area were observed to decrease 9.16% and 8.46% respectively. Velocity reduction was calculated to be significantly different for these events, $p < 0.001$. The ecological significance of the observed decrease in flow velocities in the mean annual minimum channel, designated as the spawning channel for this analysis, is discussed in the next section.

5.3 Ecological Importance

The importance of understanding the hydrology of the Greenwater River is made more apparent when analyzing changes in discharge trends over the last 10 years and how it relates to fish use. This section first outlines the different salmon species and their potential use of the project reach. Trends in peak flood occurrences are then examined.

Finally, timing of fish use is compared with flood events to highlight possible effects of flooding events on fish populations.

5.3.1 Salmon Populations

The Greenwater River is reported to support populations of Spring Chinook (*O. tshawytscha*), Coho Salmon (*O. kisutch*), and winter steelhead (*O. mykiss*) (Ecology, 1998; Marks et al., 2016). Chinook stocks in Puget Sound were federally listed as endangered in 1999, and are currently listed as threatened along with Puget Sound steelhead. Coho Salmon are common throughout the Puyallup/White River Watershed (Marks et al., 2016.). All three of these species have various life histories throughout the Greenwater River system.

Spring Chinook return to the freshwater as early as May and typically spawn in September through October (Ecology, 1998; Marks et al., 2016; WDFW et al., 1996). Egg to fry emergence occurs 90–110 days later in February through March (Ecology, 1998; Marks et al., 2016; Smith & Wampler, 1995). Most (80%) of juvenile Spring Chinook migrate as sub-yearlings out into salt water (Marks et al., 2016).

Coho Salmon enter the river system in early August with peak spawning occurring in October and November (Marks et al., 2016). These fish generally rear in the system for over a year (18 months) before entering marine waters as yearlings.

Winter steelhead, an anadromous form of rainbow trout, in the Greenwater River system generally return in November and December with peak spawning occurring in April and May (Marks et al., 2016). Egg-to-fry emergence of winter steelhead occurs 28–56 days later, depending on water temperature, and fish will rear in the freshwater river

system for 1–4 years before migrating out to salt water in the spring (Marks et al., 2016).

See figure 5.1 for StreamNet fish distributions by species, within the project reach.

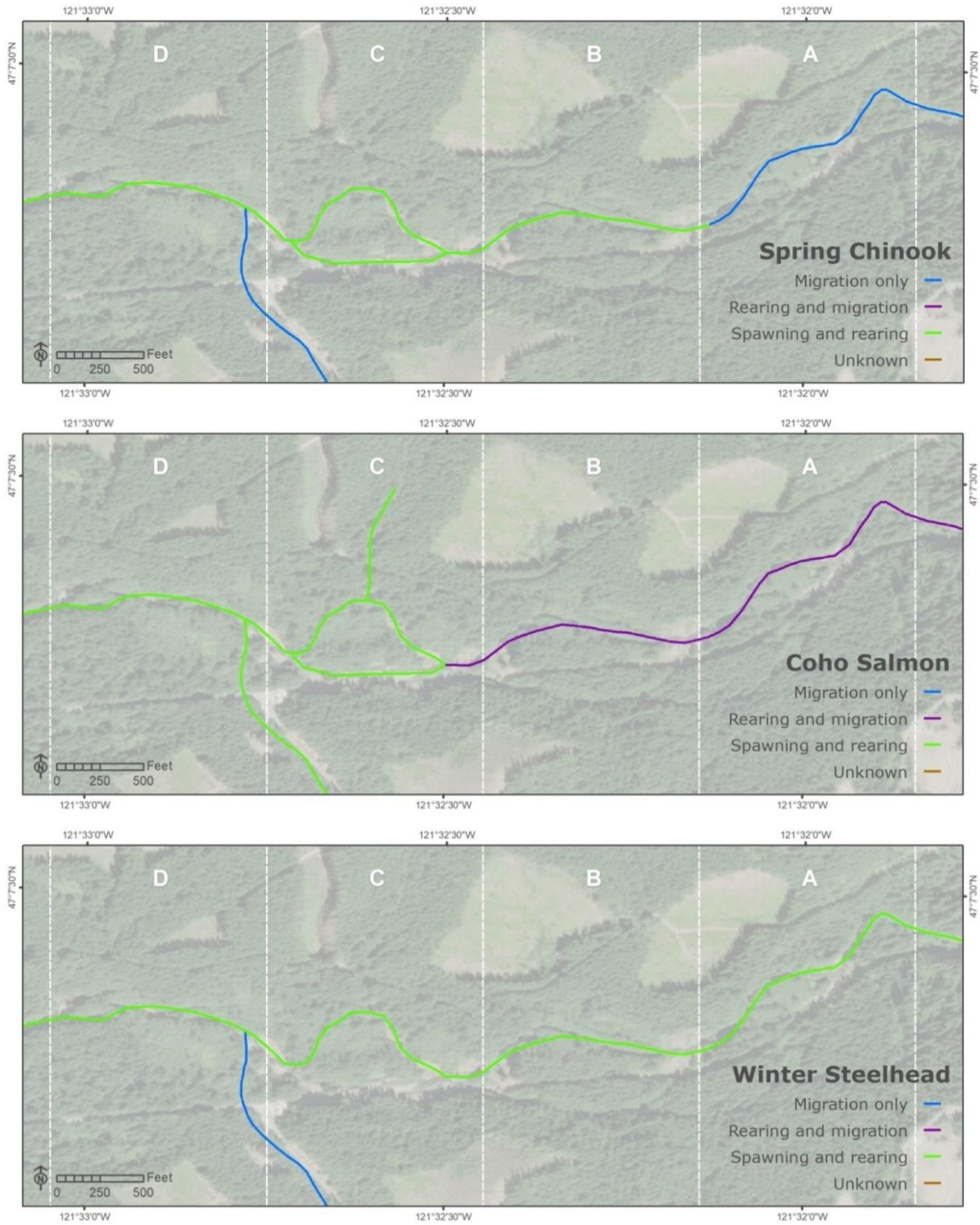
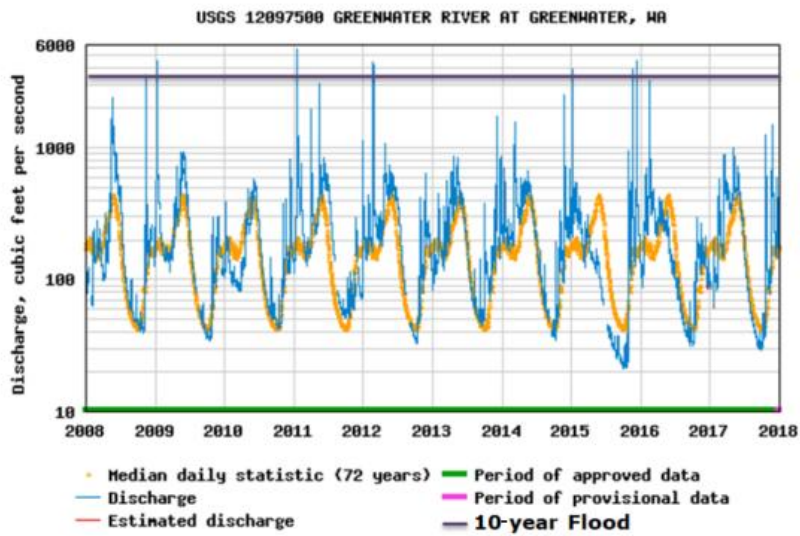
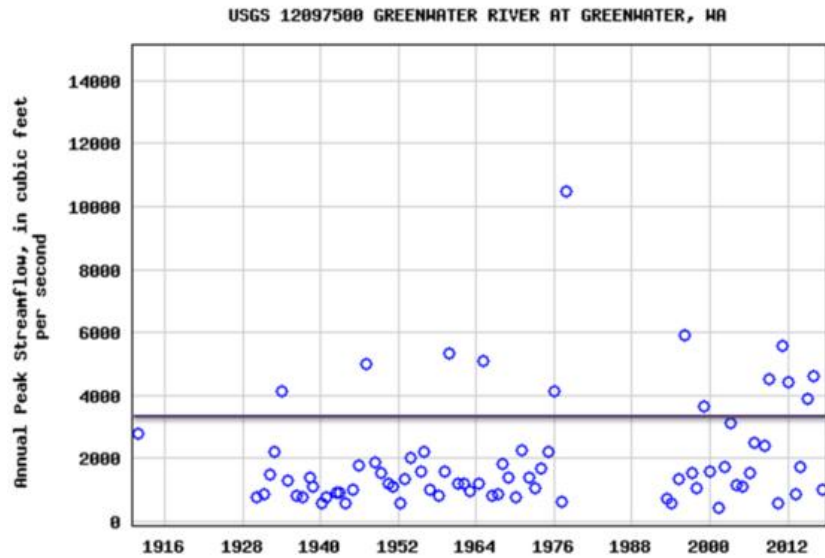


Figure 5.1. StreamNet fish distributions by species. (StreamNet GIS DATA, 2013)

5.3.2 Changes in Peak Flood Occurrence

Discharge has been regularly collected for the Greenwater River gage, no. 12097500, since 1929. Upon inspection of the USGS gage data it is observed that there has been an increase in the past decade of the number of flood events greater than the estimated 10-year event. See Figure 5.2 and Appendix C. The 10-year flood event is the peak flood level that has a 10% probability of occurring each year, with an average recurrence interval of 10 years. Within the past 10 years, there were 5 years with flood events that equaled or exceeded 10-year flood levels, with 2 years seeing multiple events greater than the 10-year flood. Prior to 2008, the average reoccurrence of the 10-year flood was once per decade, as would generally be expected. As all of these flood events occur in the winter from November to February, this is likely due to a shifting climate in which warmer temperatures are transitioning winter snowfall into rain. When rain falls on existing snowpack, both the rain and meltwaters flow downstream, amplifying the flooding effect. Alternately, as less snowpack is left in the upper watershed, decreased summer flows generally result, which can then lead to increased water temperatures during the summer months. How this relates to fish populations is discussed in the next section.



Number of Annual† Peak Flow Events above 10-year Flood per decade

1928-1937*	1938-1947	1948-1957	1958-1967	1968-1977	1978-1987**	1988-1997	1998-2007	2008-2017
1	1	0	2	1	1	1	1	5

†Annual peak flow only, does not reflect multiple flow events greater than the 10 year flood within the same year

* gage established June 1929 - No peak flow data reported for 1928-1929

** Stream gage lost during Historic Peak Flow of 10,500 cfs resulting in No Data for 14 years (1979-1992)

Figure 5.2. Annual peak streamflow 1912–2017 (top), Streamflow 2008–2017 (middle), Annual peak flow events > 10-year flood per decade (bottom)

5.3.3 Ecological Interaction

The interaction between Greenwater River salmon stocks and an increase in peak flood occurrences is visualized in Figure 5.3. Past studies have shown that decreased egg-to-fry survival rates and smolt production have been correlated with larger flood events (Beamer & Pess, 1999). Higher flows increase risk of bed scour on incubating salmon redds and can prematurely flush rearing fish out of the system.

With significant flooding events becoming more prevalent in last 10 years, particularly during Spring Chinook and Coho Salmon egg incubation months, there is a greater risk for bed scour to destroy these redds. This shift in discharge patterns is the predicted result of a changing climate transforming primarily snowmelt fed basins into transient, rain/snowmelt fed, basins, and transient basins into rainfall dominant basins (Mantua et al., 2010). Less summer snowmelt, leading to lower summer flows and increased temperatures, also increases risk to winter steelhead redds and all rearing salmon species.

In the face of a changing climate it becomes ever more important and beneficial to restore as many natural floodplains as possible to naturally increase flood storage and ease the effect of high-flow events. Restoring vegetation along riparian zones can provide needed shade, habitat complexity and eventually contribute to wood recruitment (Mantua et al., 2010). Engineered log jam placements in these projects can lead to positive wood and sediment recruitment and create more pools and protected habitat for salmon species (Cramer et al., 2012). The Greenwater River Floodplain Restoration Project adds increased resilience to the system by effectively increasing floodplain and side channel habitat while reducing flow velocities in the main channel.

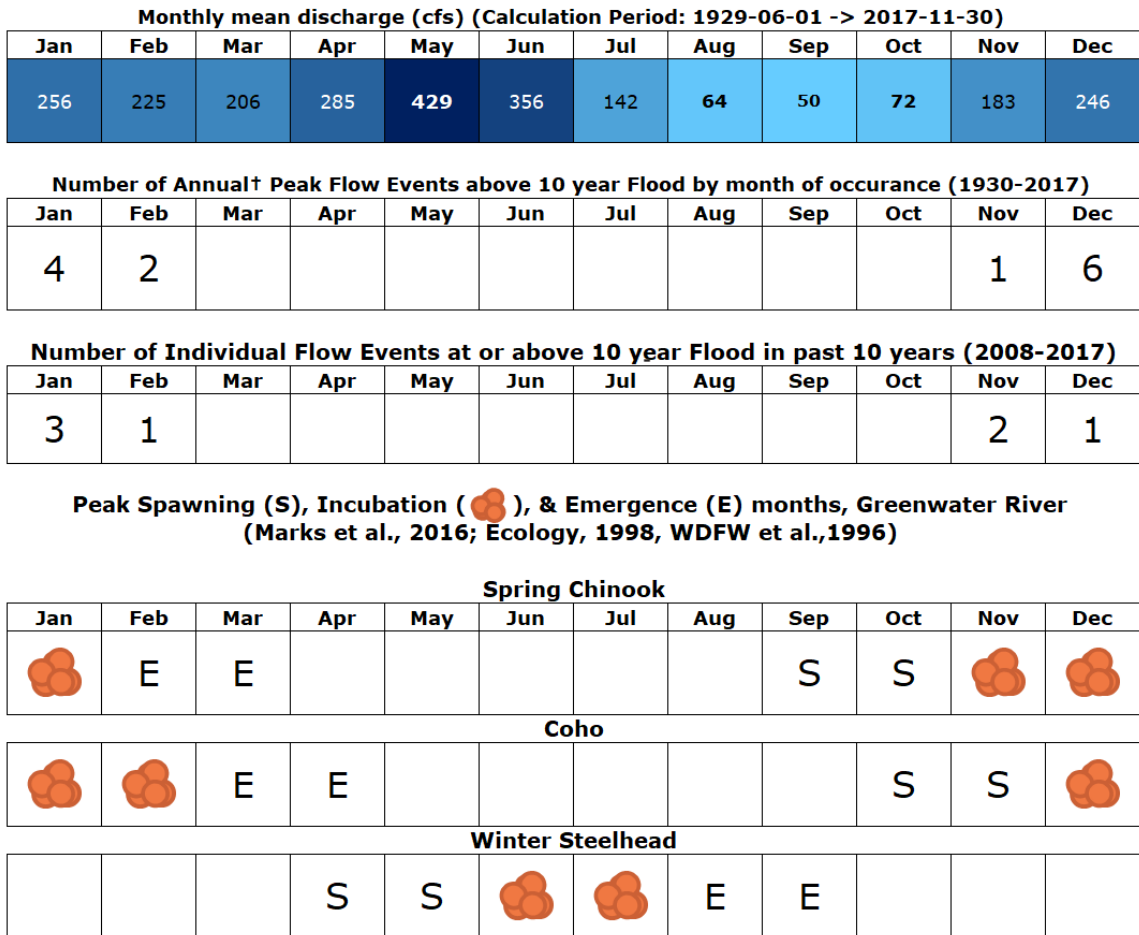


Figure 5.3. Relationship between peak flow events and salmon life histories in the Greenwater River

5.4 DTM Resolution Effect

Lidar data for post-project conditions was captured using UAV-mounted lidar, with the potential to achieve 1 cm precision with 1.5 cm accuracy. Because of heavy canopy and vegetation cover in the project area limiting the density of lidar ground returns, a 1-foot raster DTM was yielded from the bare-earth point cloud. The initial intent of this part of the research, comparing results yielded from different resolutions of the post-project data, was to examine the advantages of higher-resolution lidar data, but

this research also provided insight into the level of expected error when comparing the pre- and post-project data, with the same resolution difference.

Resolution downsampling of the 2017 terrain resulted in a relatively small change in modeled inundation area and flow velocities, with consistently smaller inundation areas modeled on the 3-foot terrain. Most of the variation between modeled inundation areas on the native and downsampled post-project terrains is observed along the banks and edges of the wetted area, with an increase in variation across the floodplain, in relatively flat areas of shallow water, where the averaging of sub-grid high and low ground features in the downsampled terrain is likely blocking shallow water flow into these areas. An increase in the percent variation is seen for the lower flow events. This is likely due to a higher ratio of effected perimeter to area of the inundation shape.

Modeled velocity comparisons for the 10 and 100-year floods reveal even less change than inundation area, showing a positive change across the whole floodplain, and a negative change within the spawning channel area. The absolute values were very small, with no change observed greater than 0.5 percent, and an average change of 0.32 percent.

While this method of downsampling the DEM is the same method used in research done by Charrier & Li (2012), it is somewhat flawed when used to output a relatively small resolution change. The downsampled DTM is still based on the same underlying higher density point cloud and the magnitude of resolution change is evidently not large enough to show a change in model results based on the averaged terrain. A more notable difference may occur if the 3-foot DTM was based on a randomly downsampled point cloud, or a separate lidar acquisition all together. Although the output

results do not warrant the higher resolution data used in this study on model output gains alone, the small change observed represents the likely small amount of error when comparing the pre- and post-project terrain data, with the same resolution difference.

The higher resolution data still have notable advantages. If captured with bathymetry data, high-resolution data could be much more useful in identifying sub-three-foot grid habitat features within the channel. The higher resolution data could also provide a more accurate representation of vegetation and other roughness factors along and above the terrain surface when analyzing these fine-scale ecological features.

5.5 Cost Benefit

A comparison of the cost difference between lidar captured by UAV or manned aircraft was also done. It can be said that for smaller project areas of only a few hundred acres the UAV lidar is less costly, although bathymetry was not available through the vender used. Larger project areas captured with a UAV would be more difficult, require multiple battery changes and ground control locations. For larger project areas, a conventional manned aircraft lidar flight would likely be more cost effective. See Table 5.1. It should be noted that the resolution of the bare-earth digital elevation model delivered from the manned aircraft lidar flight was still quoted at 3-foot resolution compared to the 1-foot resolution captured in the UAV flight.

Table 5.1. Lidar cost comparison

UAV Lidar - 1-foot resolution DEM

LiDAR Acquisition \$8,750 + Correction Points Survey \$4,227 = \$12,977 Total

Manned Aircraft Lidar Flight (quoted for the project) – 3-foot resolution DEM

<u>Green Water River, WA</u>	<u>Area (Acres)</u>	<u>Total Cost</u>
AOI 1 – NIR	1,473	\$24,550
AOI 1 - Topobathy	1,473	\$31,430
AOI 2 - NIR	146	\$23,110

5.6 Future Research

The results from this research, while they are not an exact representation of the hydrology and habitat patterns in the Greenwater River, provide a level of accuracy useful in monitoring the successes of this restoration. Typically there are methods that could improve the models and metrics used to analyze restoration efforts. Below are a few points that could further both the precision and accuracy of the predictions we make on future projects.

Roughness values, also referred to as Manning’s n values in this research, are an important part of the equations that drive the hydraulic model. Currently HEC-RAS only assigns a single roughness value to each computational grid cell face, although future versions are expected to allow for sub-grid subtlety in roughness to be expressed, similar to how sub-grid terrain is currently taken into account (Brunner, 2016). This would warrant more precise roughness determinations. The method presented by Casas et al. (2010) could then be used to more precisely parameterize roughness using the lidar data.

By capturing bathymetry data within the high-resolution terrain model a more detailed representation of instream habitat could likely be modeled and classified. This

could provide a more remote method of analysis when sending field crews in to collect habitat data is too difficult or costly.

Results from this study contribute to the body of knowledge around the effectiveness of floodplain restoration. To prioritize the best type and location of future restoration sites it would be recommended that future studies look into other river systems for similar or changing discharge trends or separation of vital functioning habitat.

6.0 CONCLUSION

Two-dimensional hydraulic modeling, utilizing HEC-RAS 5.0.3, was used in this study to evaluate the effectiveness of the Greenwater River Floodplain Restoration Project, and to provide insight into the effects and uses of higher resolution lidar-based terrain data, acquired with a UAV. Modeled results presented an increase in floodplain inundation and reduction of velocities during high flow events, providing evidence to the success of this restoration in meeting proposed restoration goals, and providing increased flood protection within the system. Collecting lidar data for this study using a UAV provided a more detailed cost-effective product than using the manned aircraft option. Although the comparison of results modeled on different resolutions of the post-project terrain yielded only small variations in spatial patterns, it is recommended that the potential uses of the higher resolution data is explored in future research, which includes the capture of bathymetric data. Results from this and other restoration monitoring projects provide a source of insight into the effectiveness of similar future projects, so that management practices can be best adapted to increase the gains of restoration.

The Greenwater River Floodplain Restoration Project was largely focused on the restoration of salmon habitat. The need for this and future restoration has become more apparent when examining the hydrology of the Greenwater River in the past ten years compared to the previous eight decades of gage flow data. In particular, it is observed that there has been an increase in 10-year peak flood occurrences in the last ten years of over 5 times the expected and historic occurrence. Shifts in the global climate, that are seen to be occurring now, have resulted in higher and more frequent flooding during

months of salmon egg incubation and rearing, and pose a risk to populations of Pacific salmon.

Continued efforts to restore and conserve rivers and streams are vital in insuring the health and survival of not only the salmon, but the rest of the ecosystem that they are an integral part of. These types of projects add both resilience and flood protection, benefiting the riverine ecosystem as well as the people who live near them. It is imperative that we continue to conduct and support the monitoring and study of these projects so that we have the information to make the most informed restoration and management decisions into the future.

REFERENCES

- Abbe, T., Beason, S., & Bunn, J. (2007). Geomorphic Basis of Conceptual Design Greenwater River Restoration Project. Prepared for South Puget Sound Salmon Enhancement Group.
- Battin, J., Wiley, M. W., Ruckelshaus, M. H., Palmer, R. N., Korb, E., Bartz, K. K., & Imaki, H. (2007). Projected Impacts of Climate Change on Salmon Habitat Restoration. *Proceedings of the National Academy of Sciences of the United States of America*, 104(16), 6720–6725.
- Beamer, E. M., & Pess, G. R. (1999). Effects of peak flows on Chinook *Oncorhynchus tshawytscha* spawning success in two Puget Sound river basins. In *Watershed Management to Protect Declining Species*. American Water Resources Association.
- Beechie, T. J., Liermann, M., Pollock, M. M., Baker, S., & Davies, J. (2006). Channel pattern and river-floodplain dynamics in forested mountain river systems. *Geomorphology*, 78(1), 124–141.
- Bernhardt, E. S., Palmer, M. A., Allan, J. D., Alexander, G., Barnas, K., Brooks, S., ... Follstad-Shah, J. (2005). *Synthesizing US river restoration efforts*. American Association for the Advancement of Science.
- Bisson, P. A., Quinn, T. P., Reeves, G. H., & Gregory, S. V. (1992). Best management practices, cumulative effects, and long-term trends in fish abundance in Pacific Northwest river systems. In *Watershed management* (pp. 189–232). Springer. Retrieved from http://link.springer.com/chapter/10.1007/978-1-4612-4382-3_7
- Box, G. E. P. (1976). Science and statistics. *Journal of the American Statistical Association*, 71(356), 791–799.
- Brakensiek, K. (2017). Greenwater River, Washington, Restoration and Monitoring -- Survey Year 2016 Update -- Summary Report. Prepared for South Puget Sound Salmon Enhancement Group.
- Brunner, G. W. (2016). HEC-RAS River Analysis System, 2D Modeling User's Manual Version 5.0. US Army Corps of Engineers Institute for Water Resources Hydrologic Engineering Center.
- Casas, A., Lane, S. N., Yu, D., & Benito, G. (2010). A method for parameterising roughness and topographic sub-grid scale effects in hydraulic modelling from LiDAR data.

- Cavalli, M., Tarolli, P., Marchi, L., & Dalla Fontana, G. (2008). The effectiveness of airborne LiDAR data in the recognition of channel-bed morphology. *Catena*, 73(3), 249–260.
- Charrier, R., & Li, Y. (2012). Assessing resolution and source effects of digital elevation models on automated floodplain delineation: a case study from the Camp Creek Watershed, Missouri. *Applied Geography*, 34, 38–46.
- Choi, Y. D. (2007). Restoration ecology to the future: a call for new paradigm. *Restoration Ecology*, 15(2), 351–353.
- Costabile, P., Macchione, F., Natale, L., & Petaccia, G. (2015). Flood mapping using LIDAR DEM. Limitations of the 1-D modeling highlighted by the 2-D approach. *Natural Hazards*, 77(1), 181–204.
- Chow, V. (1959). *Open-channel hydraulics* (Vol. 1). McGraw-Hill New York.
- Cramer, Michelle L. (managing editor). (2012). *Stream Habitat Restoration Guidelines*. Co-published by the Washington Departments of Fish and Wildlife, Natural Resources, Transportation and Ecology, Washington State Recreation and Conservation Office, Puget Sound Partnership, and the U.S. Fish and Wildlife Service. Olympia, Washington.
- Crowder, D. W., & Diplas, P. (2000). Using two-dimensional hydrodynamic models at scales of ecological importance. *Journal of Hydrology*, 230(3–4), 172–191.
- Dudley, S. J., Fischenich, J. C., & Abt, S. R. (1998). EFFECT OF WOODY DEBRIS ENTRAPMENT ON FLOW RESISTANCE 1. *JAWRA Journal of the American Water Resources Association*, 34(5), 1189–1197.
- Golshan, M., Jahanshahi, A., & Afzali, A. (2016). Flood hazard zoning using HEC-RAS in GIS environment and impact of manning roughness coefficient changes on flood zones in Semi-arid climate. *Desert*, 21(1), 24–34.
- Gresh, T., Lichatowich, J., & Schoonmaker, P. (2000). An Estimation of Historic and Current Levels of Salmon Production in the Northeast Pacific Ecosystem: Evidence of a Nutrient Deficit in the Freshwater Systems of the Pacific Northwest. *Fisheries*, 25(1), 15–21. [https://doi.org/10.1577/1548-8446\(2000\)025<0015:AEOHAC>2.0.CO;2](https://doi.org/10.1577/1548-8446(2000)025<0015:AEOHAC>2.0.CO;2)
- Herrera Environmental Consultants, Inc. (2010). *HYDRAULIC ASSESSMENT OF RESTORATION ALTERNATIVES*, Greenwater River Engineered Logjam Project. Prepared for South Puget Sound Salmon Enhancement Group.

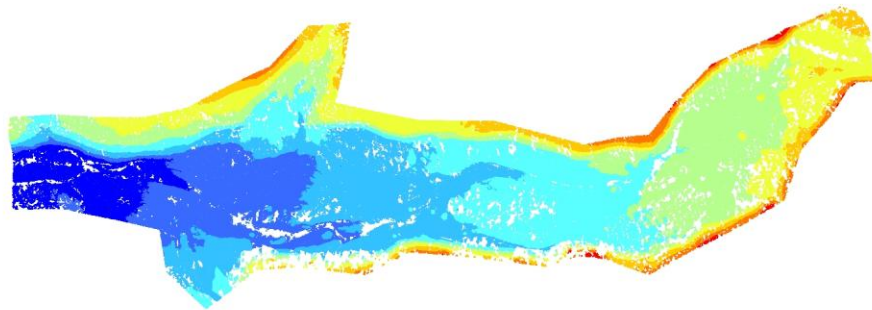
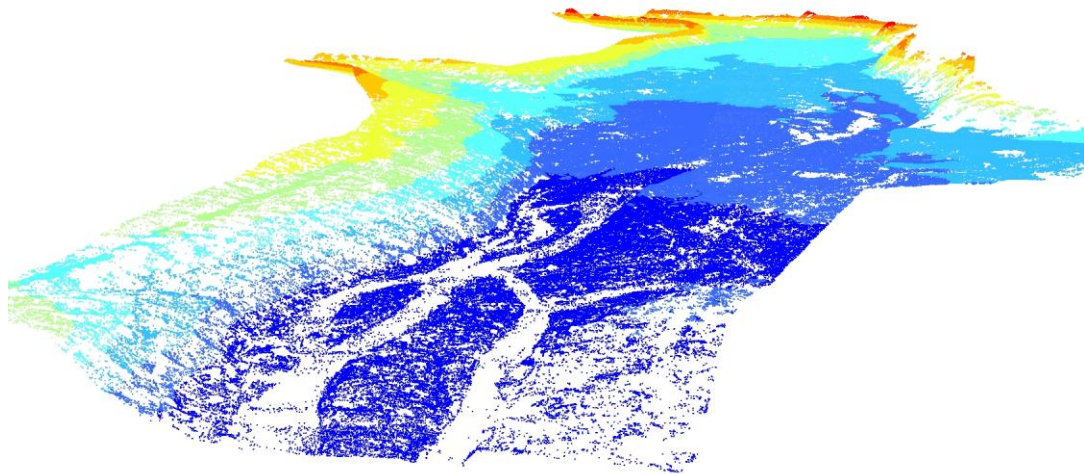
- Jeffres, C. A., Opperman, J. J., & Moyle, P. B. (2008). Ephemeral floodplain habitats provide best growth conditions for juvenile Chinook salmon in a California river. *Environmental Biology of Fishes*, 83(4), 449–458.
- Khattak, M., Anwar, F., Sheraz, K., Saeed, T., Sharif, M., & Ahmed, A. (2016). Floodplain Mapping Using HEC-RAS and ArcGIS: A Case Study of Kabul River. *Arabian Journal for Science & Engineering (Springer Science & Business Media BV)*, 41(4).
- Laurie, G.J., (2002), A Natural Channel Design to Restore the Greenwater River: Mt. Baker-Snoqualmie National Forest: U.S.D.A. Forest Service, 69 p.
- Mann, M. E., Zhang, Z., Rutherford, S., Bradley, R. S., Hughes, M. K., Shindell, D., ... Ni, F. (2009). Global Signatures and Dynamical Origins of the Little Ice Age and Medieval Climate Anomaly. *Science*, 326(5957), 1256–1260. <https://doi.org/10.1126/science.1177303>
- Mantua, N., Tohver, I., & Hamlet, A. (2010). Climate change impacts on streamflow extremes and summertime stream temperature and their possible consequences for freshwater salmon habitat in Washington State. *Climatic Change*, 102(1–2), 187–223. <https://doi.org/10.1007/s10584-010-9845-2>
- Marks, E. L., R.C. Ladley, B.E. Smith, A.G. Berger, J.A. Paul, T.G. Sebastian and K. Williamson. (2016). 2015-2016 Annual Salmon, Steelhead, and Bull Trout Report: Puyallup/White River Watershed--Water Resource Inventory Area 10. Puyallup Tribal Fisheries, Puyallup, WA.
- Mason, D. C., Cobby, D. M., Horritt, M. S., & Bates, P. D. (2003). Floodplain friction parameterization in two-dimensional river flood models using vegetation heights derived from airborne scanning laser altimetry. *Hydrological Processes*, 17(9), 1711–1732.
- McKean, J., Isaak, D., & Wright, W. (2009). Stream and riparian habitat analysis and monitoring with a high-resolution terrestrial-aquatic LiDAR.
- O’Neal, J. S., Roni, P., Crawford, B., Ritchie, A., & Shelly, A. (2016). Comparing Stream Restoration Project Effectiveness Using a Programmatic Evaluation of Salmonid Habitat and Fish Response. *North American Journal of Fisheries Management*, 36(3), 681–703. <https://doi.org/10.1080/02755947.2016.1165773>
- Quang Minh, N., & La, H. (2011). Land cover classification using LiDAR intensity data and neural network. *Korean Journal of Geomatics*, 29, 429–438. <https://doi.org/10.7848/ksgpc.2011.29.4.429>


- Quiroga, V. M., Kure, S., Udo, K., & Mano, A. (2016). Application of 2D numerical simulation for the analysis of the February 2014 Bolivian Amazonia flood: Application of the new HEC-RAS version 5. *RIBAGUA-Revista Iberoamericana Del Agua*, 3(1), 25–33.
- RCO. (2009, July). Salmon Recovery - Species Listed Under the Federal Endangered Species Act - Washington State Recreation and Conservation Office. Retrieved November 28, 2017, from http://www.rco.wa.gov/salmon_recovery/listed_species.shtml
- Reeves, G. H., Hohler, D. B., Hansen, B. E., Everest, F. H., Sedell, J. R., Hickman, T. L., & Shively, D. (1997). Fish habitat restoration in the Pacific Northwest: fish creek of Oregon. *Watershed Restoration: Principles and Practices.*, 335–359.
- Schindler, D. E., & Rogers, L. A. (2009). Responses of Pacific salmon populations to climate variation in freshwater ecosystems. In *American Fisheries Society Symposium* (Vol. 70, pp. 1127–1142).
- Smith, C. and P. Wampler, eds. (1995). Dungeness River chinook salmon rebuilding project progress report 1992-1993. Northwest Fishery Resource Bulletin No. 3. pp 1-72.
- Stewart, G. B., Bayliss, H. R., Showler, D. A., Sutherland, W. J., & Pullin, A. S. (2009). Effectiveness of engineered in-stream structure mitigation measures to increase salmonid abundance: a systematic review. *Ecological Applications*, 19(4), 931–941.
- StreamNet GIS DATA. (2013). StreamNet – Fish Distribution by Species. Retrieved from <https://www.streamnet.org/data/interactive-maps-and-gis-data/>
- Suding, K. N. (2011). Toward an era of restoration in ecology: successes, failures, and opportunities ahead. *Annual Review of Ecology, Evolution, and Systematics*, 42, 465–487.
- Thorpe, A. S., & Stanley, A. G. (2011). Determining appropriate goals for restoration of imperilled communities and species. *Journal of Applied Ecology*, 48(2), 275–279.
- USGS Current Conditions for USGS 12097500 GREENWATER RIVER AT GREENWATER, WA. (2018). Retrieved from <https://waterdata.usgs.gov/usa/nwis/uv?12097500>
- Waples, R. S., Pess, G. R., & Beechie, T. (2008). Evolutionary history of Pacific salmon in dynamic environments. *Evolutionary Applications*, 1(2), 189–206.

- Washington Department of Fish and Wildlife, Puyallup Indian Tribe and Muckleshoot Indian Tribe. (1996). Recovery plan for White River spring chinook. Washington Department of Fish and Wildlife. Olympia, WA 81p.
- Washington State Department of Ecology, Water Quality Program. (1998). White River Spring Chinook Habitat Guidance, A Water Quality Management Approach for the Upper White River.
- Watershed Sciences (2007). LiDAR Remote Sensing Data Collection: SR 410 & Greenwater River: Point, Raster and Vector Data and Data Report submitted to WSDOT Photogrammetry, Herrera Environmental Consultants and the South Puget Sound Salmon Enhancement Group, 26 p.
- Whiteway, S. L., Biron, P. M., Zimmermann, A., Venter, O., & Grant, J. W. A. (2010). Do in-stream restoration structures enhance salmonid abundance? A meta-analysis. *Canadian Journal of Fisheries and Aquatic Sciences*, 67(5), 831–841.
- Yang, J., Townsend, R. D., & Daneshfar, B. (2006). Applying the HEC-RAS model and GIS techniques in river network floodplain delineation. *Canadian Journal of Civil Engineering*, 33(1), 19–28.

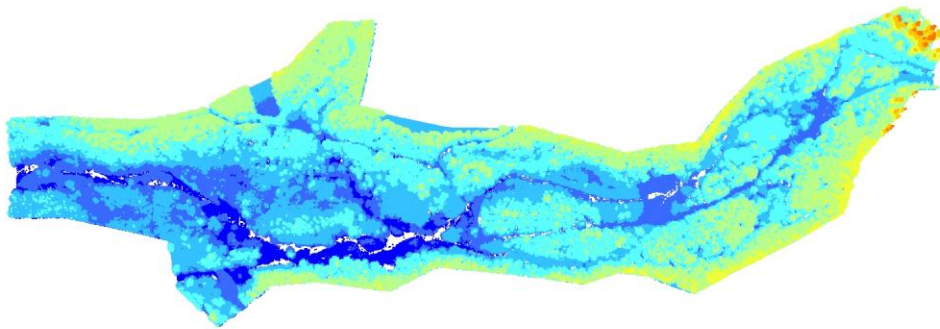
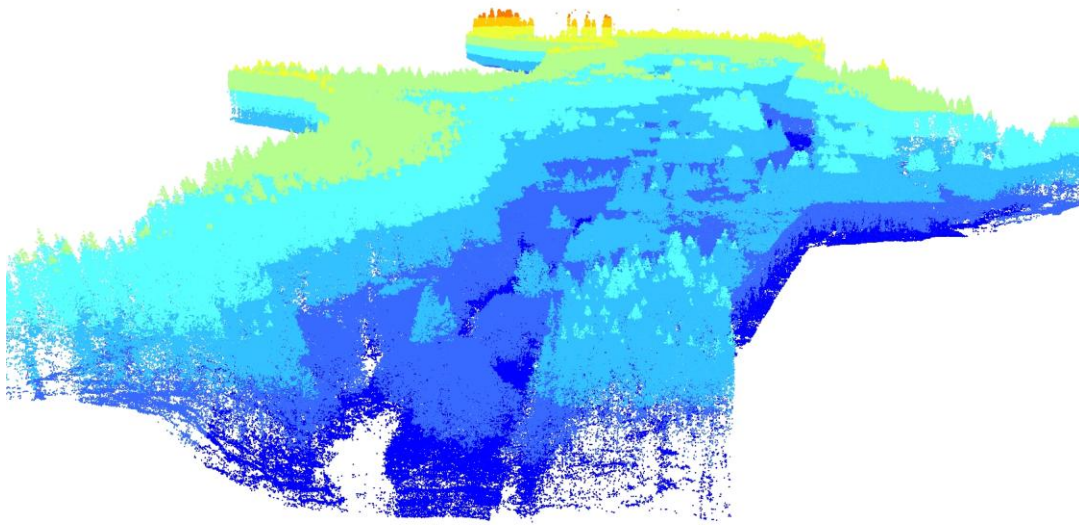
APPENDICES

Appendix A. 2017 three-dimensional lidar point cloud of bare-earth laser returns
Top: oblique view. Bottom: top down perspective



Low  High
Point Elevation

Appendix B. 2017 three-dimensional lidar point cloud of all laser returns
Top: oblique view. Bottom: top down perspective



Appendix C. Greenwater gage discharge 2008-2017

